iScience

Article

Disruption of *chrna5* blunts aversion and adaptive transcriptomic responses to nicotine and alcohol

Graphical abstract

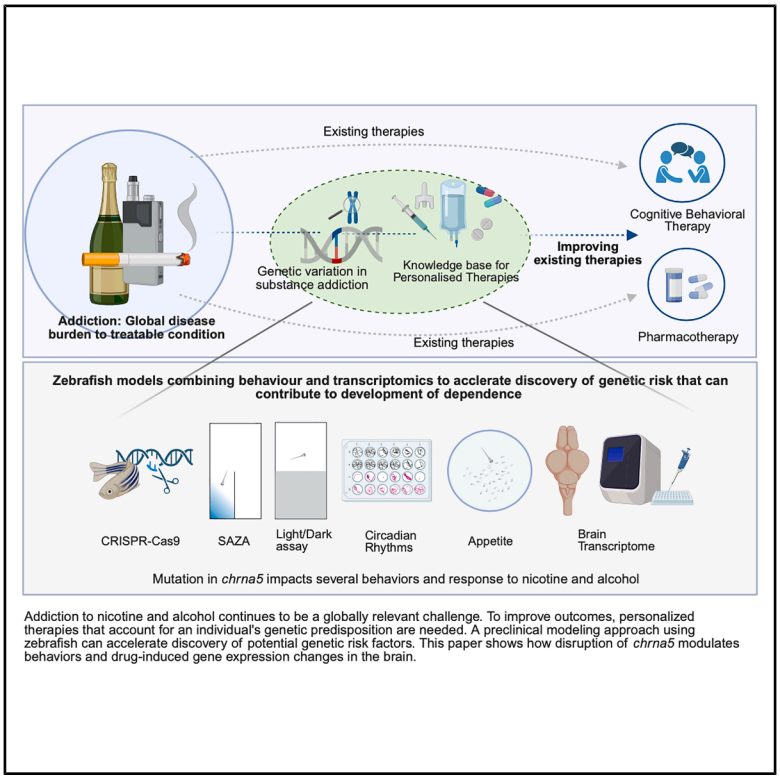

Addiction to nicotine and alcohol continues to be a globally relevant challenge. To improve outcomes, personalized therapies that account for an individual's genetic predisposition are needed. A preclinical modeling approach using zebrafish can accelerate discovery of potential genetic risk factors. This paper shows how disruption of *chrna5* modulates behaviors and drug-induced gene expression changes in the brain.

Highlights

- *chrna5* mutants showed reduced acute aversion to self-administer nicotine or alcohol
- Transcriptomic adaptation after nicotine or alcohol exposure absent in *chrna5* mutants
- *chrna5* loss altered circadian rhythms and appetite independent of drug-exposure
- Multiple brain circuits affected by mutant *chrna5* may elevate addiction risk

Authors

Tanisha Goel, Joshua Raine, Caroline Kibat, Jeff Winxin Collado, Tirtha Das Banerjee, Ajay S. Mathuru

Correspondence

ajay.mathuru@nus.edu.sg

In brief

Molecular neuroscience; Cellular neuroscience

Goel et al., 2026, iScience *29*, 114735
February 20, 2026
https://doi.org/10.1016/j.isci.2026.114735

CellPress

iScience

CellPress
OPEN ACCESS

Article

Disruption of *chrna5* blunts aversion and adaptive transcriptomic responses to nicotine and alcohol

Tanisha Goel,[1,8] Joshua Raine,[1,8] Caroline Kibat,[1] Jeff Winxin Collado,[2] Tirtha Das Banerjee,[3] and Ajay S. Mathuru[1,2,4,5,6,7,9,*]

[1]Department of Physiology, Yong Loo Lin School of Medicine, National University of Singapore, Singapore, Singapore
[2]Yale-NUS College, National University of Singapore, Singapore, Singapore
[3]Department of Biological Sciences, National University of Singapore, Singapore, Singapore
[4]N.1 Institute for Health, National University of Singapore, Singapore, Singapore
[5]Institute of Digital Medicine (WisDM), Yong Loo Lin School of Medicine, National University of Singapore, Singapore, Singapore
[6]Institute of Molecular and Cell Biology, A*STAR, Singapore, Singapore
[7]Healthy Longevity Translational Research Programme, Yong Loo Lin School of Medicine, National University of Singapore, Singapore, Singapore
[8]These authors contributed equally
[9]Lead contact
*Correspondence: ajay.mathuru@nus.edu.sg
https://doi.org/10.1016/j.isci.2026.114735

SUMMARY

Addiction to nicotine and alcohol continues to be a leading cause of death and loss of productivity. Polymorphisms in *CHRNA5* have been identified as risk factors in human genetic studies. Whether the *CHRNA5* function is independently relevant to phenotypes associated with substance abuse and if genetic factors influence subsequent outcomes when exposure to psychoactive substances happens at an early age, are questions of interest. We generated a stable mutant line in zebrafish using the CRISPR-Cas9 technique. We found the *chrna5*-mutant fish exhibited an increased acute preference to both nicotine and alcohol in the self-administration zebrafish assay (SAZA). When subjected to multi-day exposures to either drug, *chrna5* mutants exhibited greater behavioral changes, but reduced transcriptomic changes compared with wild-type siblings, suggesting an impaired homeostatic regulation following drug exposure. *chrna5* mutants also exhibited drug-independent changes in appetite and circadian rhythms. We expect these results to give new insights into genetic predisposition that modulates vulnerability to nicotine and alcohol abuse.

INTRODUCTION

Substance use disorders (SUDs), due to the abuse of nicotine, alcohol, or opioids, continue to have a substantial impact across socio-economically diverse populations globally and among young adults.[1–3] The direct death toll from tobacco alone is predicted to exceed 8 million per year by 2030,[4,5] with cancers, cardiovascular diseases, and chronic obstructive pulmonary disorders as the major disease outcomes.[6] The development of dependence leading to these outcomes is a multifold mix of socio-economic, cultural, neurobiological, and genetic factors that is challenging to untangle.[7,8]

A particularly vulnerable period of substance exposure is early age, when the still-developing brain undergoes significant neurodevelopmental and neuroanatomical changes. Exposure during this critical window can lead to profound alterations in brain structure and gene expression that can be long-lasting.[9,10] Genetic variation contributes to differences in individual susceptibility, both for the consequences of exposure at an early age and the risk of developing SUDs subsequently.[9] Research aimed toward isolating the genetic components has revealed strong associations between polymorphisms in nicotinic acetylcholine receptor subunit genes (nAChRs) and nicotine use.[11] In particular, the gene cluster *CHRNA5-CHRNA3-CHRNB4* encoding for the α5, α3, and β4 subunits has been frequently identified in genome-wide association studies.[12–17]

In rodents, where *Chrna5* function has been examined extensively,[18] expression across many regions of the brain, including the medial habenula-interpeduncular nucleus (IPN) pathway[19] and the ventral tegmental area (VTA[20]) is documented. These regions are proposed to impact avoidance behaviors, withdrawal, and nicotine dependence.[21] Manipulation of *Chrna5* levels within them has been shown to alter nicotine preference.[19,22] In addition to nicotine, polymorphisms in the *CHRNA5-CHRNA3-CHRNB4* locus have also been correlated with vulnerability to alcohol dependence,[23,24] despite alcohol not being a direct ligand.[24–27] As co-abuse of nicotine and alcohol is common,[28] elucidation of the interdependent relationships represents an important step toward conceiving holistic interventions. Multi-day exposure to nicotine and alcohol impacts both the transcriptional profile and behavior, and it is equally important to understand the neuroadaptive changes in the brain that influence

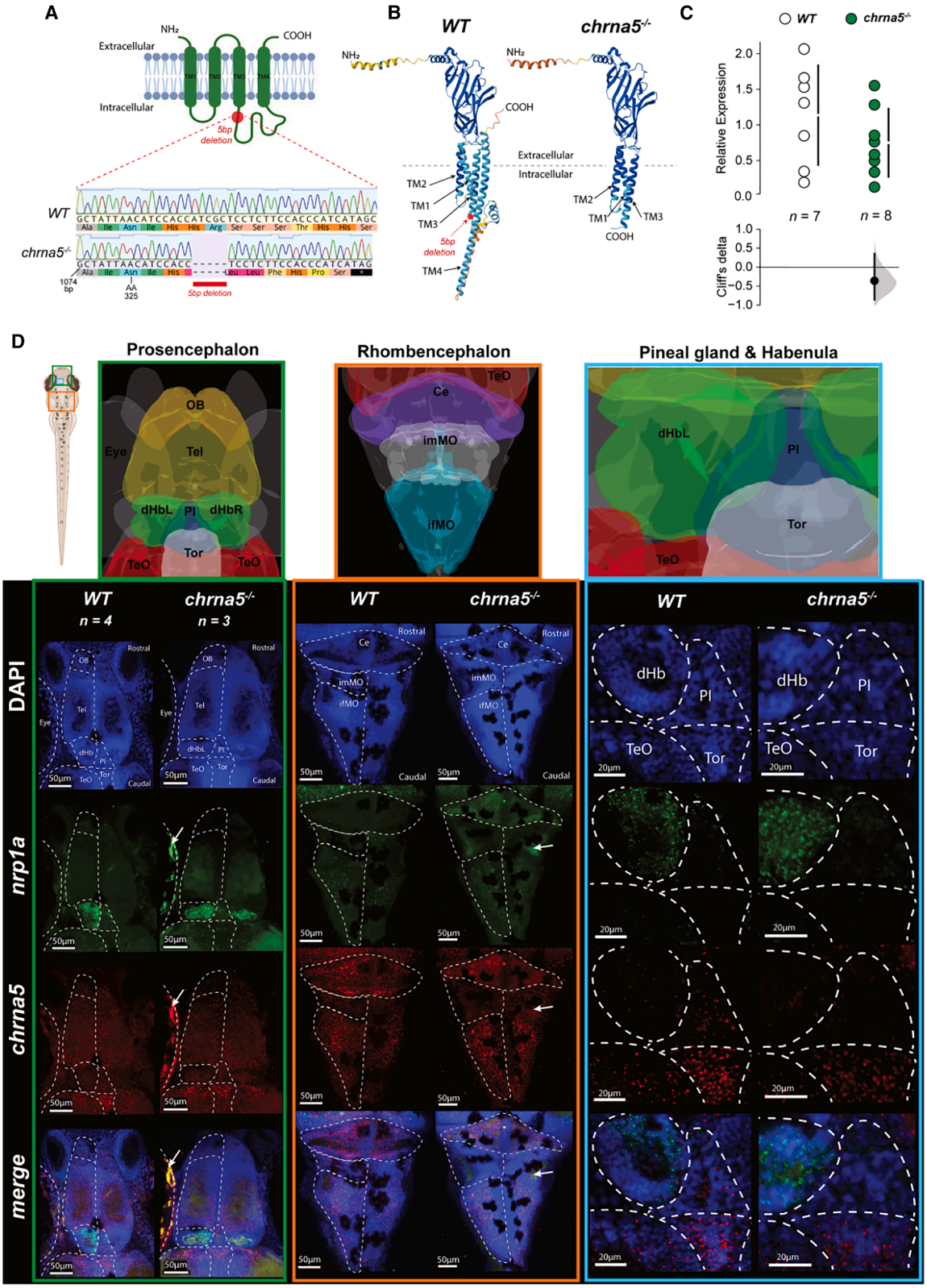

(legend on next page)

behavior.[29–31] Furthermore, the harmful outcomes of SUDs are not limited to addiction, as neurophysiological disorders of anxiety, sleep, and appetite control often occur comorbidly in humans.[32] Therefore, understanding the mechanisms underlying the initial stages of dependence, at an age when brains are still developing, is crucial for the design of interventional strategies informed by genetic predisposition.

Untangling the contribution of genetic predisposition to the induction of these disorders is challenging to discover in humans, however, due to the bidirectional nature of the relationships between drug use and neuroplasticity, and ethical considerations such as assigning an adolescent to drug exposure in a randomized control trial. In this context, animal models can be effective intermediates to bridge the gap in our knowledge. In addition to the mammalian models, the zebrafish (*Danio rerio)* represents a viable alternative to study neurogenetics, thanks to the established conservation of function and anatomy,[33–35] cost effectiveness, efficient genetic manipulation, and live, whole brain neural activity imaging.[36] At the same time, a battery of behavioral assays to rapidly examine anxiety-like behaviors,[37] circadian rhythms,[38] and appetite[39] are now available. New assays to examine not just the effect of psychoactive substances,[40] but also the natural responses[41–44] add to their value for neurogenetic studies.

Here, we generated a zebrafish *chrna5* mutant line using CRISPR-Cas9 technique to study transcriptomic and behavioral change after exposure to substances of abuse at an early age. In drug preference assays, homozygous *chrna5* mutant juvenile fish phenocopied adult rodent responses, exhibiting increased acute, naive self-administration of both nicotine and alcohol. This recapitulation validates the use of this model system to study the neurogenetics of the development of SUDs. Multi-day, pre-exposure experiments revealed the modulation of preference, with greater influence on *chrna5* mutant behavior, while homeostatic transcriptomic changes reduced behavioral changes in WT animals. *chrna5* mutants were also impaired in circadian rhythm and appetite regulation, with no effect on anxiety-like behaviors. This study thus adds to our knowledge of α5 nicotinic acetylcholine receptors in the development of SUDs and the potential consequences of manipulating their function as an intervention.

RESULTS

Molecular characterization of *chrna5* mutant

The *chrna5* mutant zebrafish generated for this study by CRISPR-Cas9 technique had a five-base pair deletion in exon 8, resulting in a premature termination codon at amino acid position 334 (Figure 1A, Table 1). This stop codon was predicted to truncate the protein at the intracellular loop between the third and fourth transmembrane regions (Figure 1B). Quantitative RT-PCR of the whole brains suggested that the abundance of the *chrna5* transcript was stable till adulthood in the mutants, with only a small, non-significant reduction in expression (Figure 1C, Table 2), *chrna5* vs. WT (Cliff's delta = −0.438, 95CI [0.156, −0.875], $p = 0.122$). There was, however, a reduction in the relative abundance of Chrna5 protein levels in adult brains (Figure S7). *Chrna5* in mice is co-expressed with *Chrna3* and *Chrnb4* in the habenula-IPN circuit.[11,18] Therefore, we also examined expression of these genes by RT-qPCR. Expression of *chrna3* and *chrnb4* was also unchanged in the mutant brains (Figure S1).

In zebrafish, *chrna5* mRNA expression has been reported in the habenula, the ventral, and ventral intermediate IPN as well as in the telencephalon.[47,48] Chrna5 protein expression was reported to be broader in a recently established transgenic line; in the pineal gland, stratum periventricular of the optic tectum, corpus cerebellum, hindbrain motor neurons, and the spinal cord.[49] Therefore we examined *chrna5* expression in the whole brain using a recently developed RAM-FISH technique that allowed for spatial transcript analysis to be conducted in intact 14 day post-fertilization (dpf) zebrafish.[50] This experiment revealed that indeed, *chrna5* expression can be seen in many neurons in the telencephalon, torus longitudinalis, cerebellum, spinal area, while the hindbrain exhibited the highest relative expression (Figures 1D, S2, S3, and S6). Low levels of expression were also seen in the dorsal habenula (Figure 1D). However, there were no qualitative or quantitative differences observable in the mutants. Evaluation of other genes commonly associated with specific habenula sub-regions, such as *kiss1*, *nrp1a*, and *gpr139* also had similar expression across the two genotypes (Figures S4 and S5).

Self-administration for zebrafish assay to examine acute response to nicotine and alcohol

Given the strong links reported between loss-of-function *chrna5* mutations, or knockouts, and altered intake of nicotine and alcohol in rodents,[19,22,25] we first examined if zebrafish *chrna5* mutants also showed similar response change to nicotine and alcohol in spite of the evolutionary distance to mammals. To do so, we used the previously developed self-administration for zebrafish assay (SAZA).[41,44] SAZA allowed juvenile zebrafish an uninhibited choice to self-administer a stimulus, contingent on fish swimming into a stimulus dispensing zone of the assay

Figure 1. Characterization of *chrna5* mutant zebrafish

(A) Schematic representation of Chrna5 transmembrane helices. The red line indicates the stop codon present in the mutants between the third and fourth transmembrane regions. Mutants had a 5bp deletion in exon 8 at position 10, resulting in a premature termination codon at amino acid 334 (UniProt: Q567Y7_DANRE).

(B) Predicted tertiary protein structure of Chrna5 in WT and Chrna5 mutants, generated by Alphafold.[45]

(C) Fold change (± standard deviation) of *chrna5* mRNA in *chrna5* mutants ($n = 8$) vs. WT ($n = 7$) whole brain tissue by qPCR. See Table S10 for the precise effect size and p values.

(D) Gene expression patterns in WT ($n = 4$), and *chrna5* mutant ($n = 3$), 14 dpf larval zebrafish brains visualized by HCR RNA-FISH (HCR). Schematic images with regional markers (v2.0, MECE, 2024) were generated in mapZeBrain Atlas (mapzebrain.org, Jan 2025).[46] OB = olfactory bulb, Tel = telencephalon, Hb = habenula, dHb = dorsal habenula, dHbL = left dorsal habenula, dHbR, right dorsal habenula, Pl = pineal gland, Tor = torus longitudinalis, TeO = optic tectum, Ce = cerebellum, imMO = intermediate medulla oblongata, ifMO = inferior medulla oblongata. Scale bars, prosencephalon = 50 μm, rhombencephalon = 50 μm, pineal gland and habenula = 20 μm. Non-specific background in the eye and hindbrain denoted by white arrows. See also Figures S2, S3, S6, and S7.

chamber (Figure 2A). During SAZA characterization, the stimuli dispensed into the assay chamber were measured to be diluted by ~25 to 70 fold for alcohol,[44] and estimated by ~10 to 40 fold for nicotine (Table S2). Hence, 10 and 500 μM nicotine at source were diluted to estimated mean concentrations of x̄0.5 μM and x̄25 μM (Table S2), while 5%, 10%, and 20% alcohol at the source were diluted to an average concentration of x̄0.125%, x̄0.25%, and x̄0.5%, respectively.[44] These terms are used for the remainder of the work. The experimental design had a pre and post-stimulus period interspersed with an 18 min self-administration period (Figure 2A). Several parameters of the behavior were quantified as described in the methods. Among these the preference index (PI) was calculated as the relative preference for the stimulus compared to the control based (Figure 2A). Thus, positive PI values (0 to +1) indicated preference for the stimulus, while negative PI (0 to −1) indicated an aversion.

chrna5 mutants exhibit reduced aversion to nicotine

WT fish showed a pronounced aversion to nicotine that increased with dispensing concentration (Figure 2B x̄25 μM, Cliff's delta = −0.762, 95% CI [−0.900, −0.533], $p < 0.001$). In contrast, this aversive response was absent in *chrna5* mutants: the PI at both x̄0.5 and x̄25 μM did not differ from fish self-administering 0 μM nicotine (Figure 2C). This reduced aversion in *chrna5* mutants was also evident relative to WT at both concentrations, with the largest effect at the higher concentration (Figure 2D, x̄25 μM, Cliff's delta = 0.493, 95% CI [0.704, 0.202], $p = 0.0036$). We also estimated nicotine absorption during the acute self-administration assay by measuring body cotinine. These estimates suggested levels in the range of ~0.75–2.5 μM nicotine within the assay duration (Figure S8 and Table S3). Overall, these results indicate that the mutation blunted the aversive response, especially at higher nicotine concentrations.

chrna5 mutants exhibit reduced aversion to alcohol

Alcohol also evoked an overall aversive response in WT fish, becoming notable at the highest concentration (Figure 2G x̄0.5%, Cliff's delta = −0.611, 95% CI [-0.810, −0.327], $p < 0.001$). In contrast, *chrna5* mutants exhibited attraction at x̄0.125% and x̄0.25%, as indicated by positive PI relative to the 0% alcohol SAZA (Figure 2H x̄0.125%, Cliff's delta = 0.447, 95% CI [0.121, 0.691], $p = 0.0068$, x̄0.25% Cliff's delta = 0.444, 95% CI [0.131, 0.665], $p = 0.0054$). Unlike WT, aversion was not observed in the mutants at the highest concentration (Figure 2H x̄0.5%, Cliff's delta = −0.109, 95% CI [-0.181, 0.399], $p = 0.4654$). Inter-genotype comparisons highlighted this large effect differentiating mutants from WT at x̄0.5% (Figure 2I x̄0.50%, Cliff's delta = 0.430, 95% CI [0.135, 0.667], $p = 0.0184$). We quantified the body alcohol content that fish likely experienced during the assay using a method previously used.[51] These estimates suggested body alcohol levels in the range of 0.026%–0.036% at the highest concentration during the assay (Figure S9 and Table S4).

chrna5 mutants do not exhibit overt locomotion deficits

While some inter-genotypic differences in velocity were noted, these were similar across the entire arena for both nicotine and alcohol (Figure S11 and Table S5). Additionally, both genotypes showed a similar, weak correlation between time spent in the stimulus zone and velocity outside the stimulus, indicating that locomotor stimulation or sedation due to nicotine or alcohol exposure was unlikely to account for the genotypic differences in preference indices (Figures S12 and S13 and Tables S6–S9). Importantly, WT and *chrna5* mutant fish locomotion was mostly comparable in the absence of nicotine or alcohol, indicating that the *chrna5* mutation had limited influence on normal behavior in the SAZA apparatus (Figures S11A, S11B, S11E, and S11F). Examining the time spent in the stimulus zone into 3-min windows revealed that mutants also showed an aversive response to nicotine resembling WT, but at a later time, or with a delayed onset (Figures S10A and S10B). Meanwhile, as the acute response to alcohol in SAZA is biphasic,[44] aversion to it emerged in WT primarily in the latter half of the assay (Figure S10C). If a similar delay in alcohol aversion occurred in the mutants, it fell outside the assay duration (Figures S10C and S10D).

In the presence of either nicotine or alcohol, however, other behavioral metrics supported the observation of a blunted aversion in the mutant (Figures 2E, 2F, 2J, and 2K). Under x̄25 μM nicotine, WT fish spent less time in the stimulus zone and made fewer entries relative to the 0 μM condition, while *chrna5* mutants showed no change (Figures 2E and 2F). Similarly, in the x̄0.5% alcohol condition, WT fish reduced time in the stimulus zone and mean time per entry versus baseline, whereas mutants again showed no change (Figures 2J and 2K). In all cases, changes in mean velocity were observed, indicating that even the small duration of 2–3 min of substance exposure was enough to affect the animals (Figures 2J and 2K). These results together suggest that *chrna5* zebrafish mutants exhibited a phenotype of reduced aversion to substances of abuse like nicotine and alcohol, in line with the observations made in *chrna5*-mutant rodent studies.

Multi-day nicotine and alcohol exposure modulates behavior and brain transcript profile

We next evaluated the impact of mutation on substance use dynamics. To do so, we examined the effect of multi-day exposures on self-administration preference, as substance abuse happens after recurring exposure to these stimuli that can alter both gene expression and behavior.[30,52] Furthermore, as nicotine addiction and alcohol abuse often co-occur in humans,[53,54] we also examined cross-treatment effects (Figure 3A). To examine all these aspects, we designed a multi-day substance exposure scheme before examining gene expression or behavioral changes. Thus, we used a 2 × 2 scheme, where WT and *chrna5* mutants were subjected to a one-week pre-treatment with either nicotine or with alcohol prior to behavioral studies in the SAZA, and transcriptome analyses as outlined in Figure 3.

Nicotine pre-treatment reduced nicotine self-administration in *chrna5* mutants

Following pre-treatment with nicotine, WT fish exhibited aversion when self-administering nicotine (Figure 4A). In the forest plots (Figures 4, 5A, 5B, 5D, and 5E), aversive behaviors could be characterized by PI, time in stimulus, number of entries to the stimulus zone, and mean time per entry, all exhibiting negative values when compared to 0 μM SAZA (Figure 4A PI, Cliff's

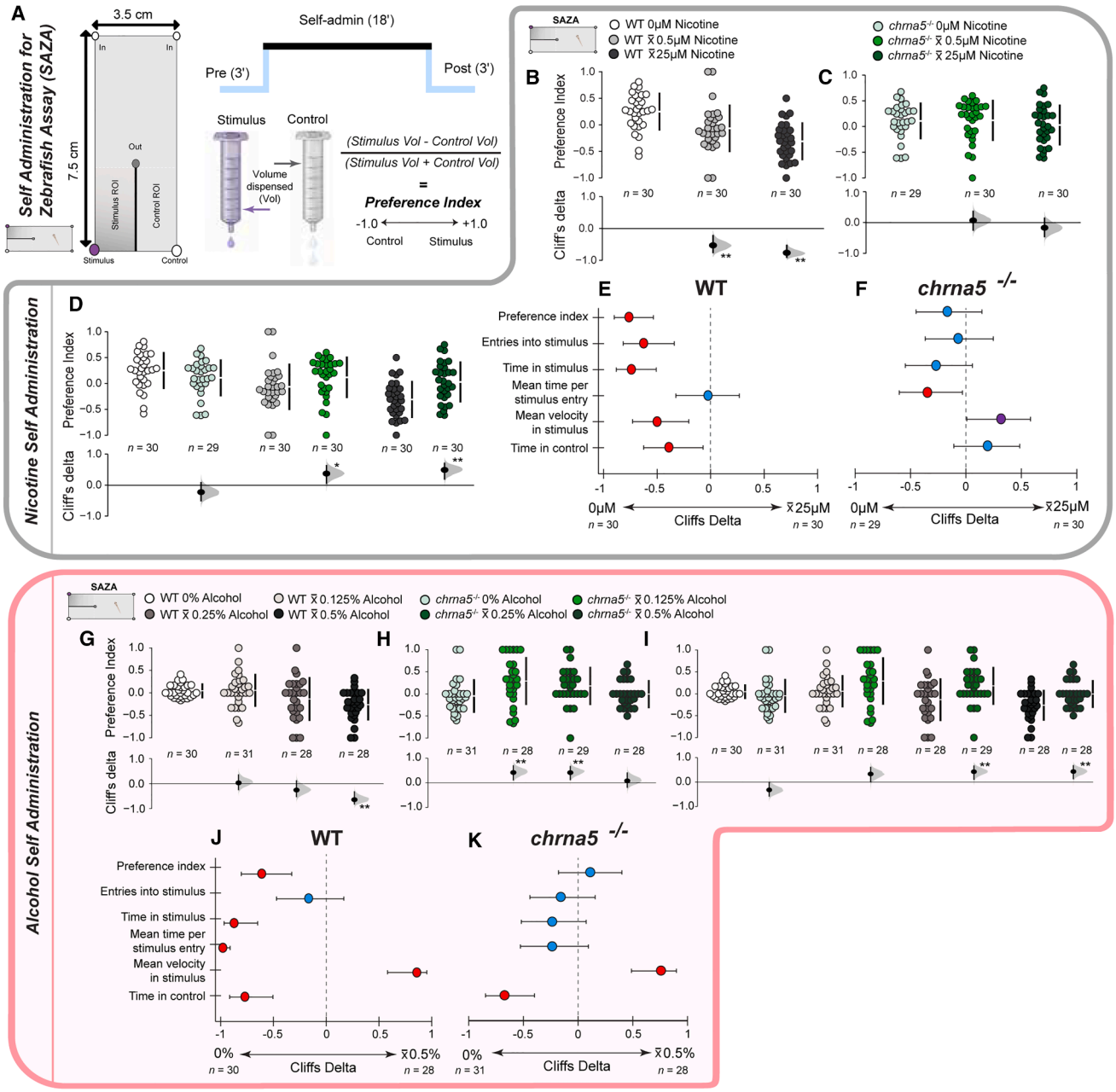

Figure 2. Zebrafish with *chrna5* mutation exhibited reduced aversion to acute nicotine & alcohol exposure by SAZA

No significant difference was observed between genotypes in the absence of drugs.

(A) Schematic of the self-administration for zebrafish assay (SAZA) chamber and design.

(B–D, G–I) Gardner-Altman and Cumming estimation plot dose-response curves displaying preference index (PI, (± standard deviation) by relative volume dispensed per fish of (B–D) 0-x̄25 μM nicotine, or (G–I) alcohol, within (B and G) WT (greys), (C and H) *chrna5* mutant (greens), or (D and I) between genotypes. Data represented as preference Index (±95% CI). In the Gardner-Altman plots (B–D, G–I) positive PI values (toward +1) indicate preference for the stimulus, negative values (toward −1) indicate preference for the control, and 0 is neutral, showing no preference for stimulus or control. (E–F, J–K) Cliff's delta (±95% CI) forest plots of all calculated metrics from (E and F) nicotine and (J and K) alcohol SAZA, comparing the response of (E and J) WT or (F and K) *chrna5* mutants to their baseline behavior within genotype. In the forest plots (E, F, J, and K), positive Cliff's delta values (to the right, +1) indicate a greater response in the treated condition, negative values (to the left, −1) indicate a greater response in the untreated condition, and values closer to the center (0), show equal responses between the two conditions. Fish numbers as follows, WT nicotine, 0/x̄0.5/x̄25 μM, *n* = 30/30/30; *chrna5*$^{-/-}$ nicotine, 0/x̄0.5/x̄25 μM, *n* = 29/30/30; WT alcohol, 0/x̄0.125/x̄0.25/x̄0.5%, *n* = 30/31/28/28; *chrna5*$^{-/-}$ alcohol, 0/x̄0.125/x̄0.25/x̄0.5%, *n* = 31/28/29/28. Asterisks (B–D, G–I), or color (E, F, J and K) indicate a significant difference:/blue = $p > 0.05$ (no significant difference), */purple = $p < 0.05$ and Cliff's delta > ± 0.2 and < ± 0.4 (provisional difference), **/red = $p < 0.01$ and Cliff's delta > ± 0.4 (meaningful difference). See Tables S11 and S12 for the precise effect sizes and *p* values, corrected for multiple comparisons between treatments against 0 μM/0% (B, C, G, and H) or genotypes against WT (D and I). See also Figures S8 and S9.

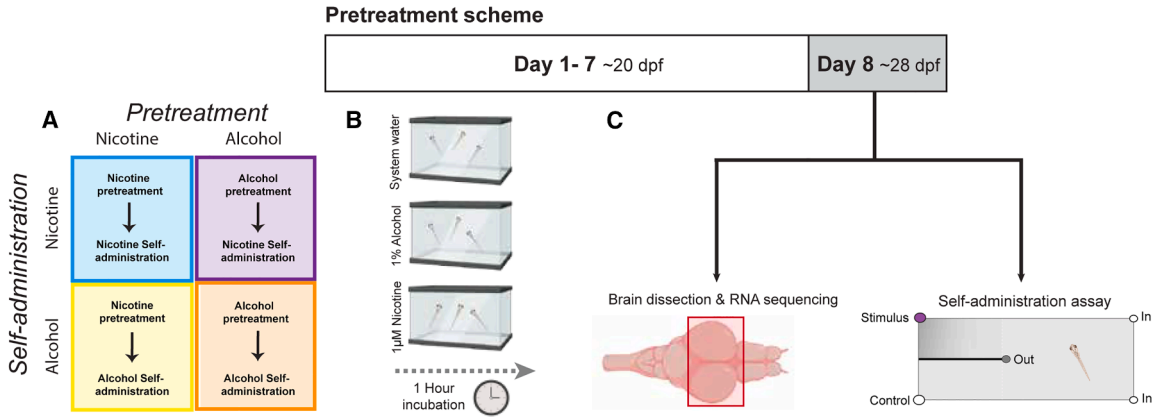

Figure 3. Combined multi-substance behavioral and transcriptomic analysis schematic

Schematic detailing (A) pre-treatment and self-administration combinations, (B) the pre-treatment schemes for alcohol and nicotine repeated daily over seven days, and (C) the analyses performed on the pre-treated fish.

delta = −0.792, 95% CI [−0.917, −0.572], $p < 0.001$). This behavioral profile remained consistent with the untreated, naive fish response (Figure 2E). *chrna5* mutants on the other hand exhibited a negative PI and time spent in stimulus in the x̄25 μM nicotine SAZA following nicotine pre-treatment, when compared to the 0 μM SAZA (Figure 4B PI, Cliff's delta = −0.414, 95% CI [-0.667, −0.0989], $p = 0.0058$). This contrasts with the response of the untreated, naive mutants (Figure 2F). This behavioral shift resulted in a narrower phenotypic gap between the two genotypes (Figure 4C pre-treated mutant vs. pre-treated WT, Cliff's delta = 0.338, 95% CI [0.0258, 0.578], $p = 0.0244$). This suggests that nicotine pre-treatment exhibited aversion in both WT, and mutants. Whether this was due to a true lack of change in phenotype in the WT fish or if the lower bounds to quantify avoidance behaviors in the SAZA had already been reached, require additional lines of experimentation.

Nicotine pre-treatment increased alcohol self-administration in both genotypes

Following pre-treatment with nicotine, WT fish exhibited a weaker aversive response to self-administering alcohol compared to their response to 0% alcohol (Figure 4D PI, Cliff's delta = −0.383, 95% CI [−0.637, −0.0713], $p = 0.011$). This contrasted with the strong aversion to alcohol observed in naive animals (Figure 2J). Meanwhile, the *chrna5* mutant fish exhibited a preference for x̄0.5% alcohol following nicotine pre-treatment, indicated by the positive effect size when compared to those in 0% SAZA (Figure 4E PI, Cliff's delta = 0.335, 95% CI [0.0516, 0.587], $p = 0.0252$). This is also a change from the untreated *chrna5* mutants, which displayed a neutral preference to alcohol in x̄0.5% SAZA (Figure 2K). Overall, this suggests that cross-pre-treatment with nicotine shifted the alcohol response rightwards, such that the aversion was reduced in WT, and the mutants exhibited a preference.

Nicotine pre-treatment changed the transcriptional profile of WT, but not *chrna5* mutants

Next, we performed bulk RNA-sequencing on the brains of juvenile fish that had undergone nicotine pre-treatment to explore potential transcriptomic changes underlying these behavioral shifts. Untreated WT and *chrna5* mutant fish showed few transcriptomic differences (Figures S15 and S16). While untreated and pre-treated samples were separated in the PCA for both genotypes (Figures 4G and 4M), nicotine pre-treatment of *chrna5* mutants appeared to effect fewer transcriptomic changes than in WT (Figures 4H and 4N). Nicotinic acetylcholine receptor subunit expression was unchanged in either genotype (Figures 4I and 4O). Interestingly, several genes in the glutamate, GABA, and dopamine receptor families were significantly downregulated in the WT fish, which were absent in the mutants (Figures 4J–4L and 4P–4R).

Alcohol pretreatment did not alter alcohol response

We next examined the self-administration behavior of fish pre-treated with alcohol. WT fish avoided x̄0.5% alcohol (Figure 5A PI, Cliff's delta = −0.617, 95% CI [−0.799, −0.347], $p < 0.001$). This paralleled the strong aversion seen in naive, untreated fish (Figure 2J). On average, *chrna5* mutants did not exhibit either an aversion or a preference to x̄0.5% (Figure 5B). This result appeared to be similar to the response of untreated mutants (Figure 2K). However, the intergenotypic comparison revealed that the differences observed between WT and mutants in the untreated condition had diminished (Figure 5C) mutant vs. WT pre-treated, Cliff's delta = 0.225, 95% CI [−0.0927, 0.504], $p = 0.1302$). This appeared to be due to an increase in the variance in individual PI of the mutants, with a greater variation in the distribution of both positive and negative preference indices.

Alcohol pretreatment increased nicotine aversion in *chrna5* mutants

Finally, we examined the effects of cross-treatment on self-administration as well. Alcohol pre-treated fish were given the choice to self-administer x̄25 μM nicotine. WT fish in this condition showed a strong aversion to nicotine entering the stimulus zone fewer times, and spending less time in the stimulus zone compared to their response to 0 μM nicotine (Figure 5D). The *chrna5* mutants also showed an aversion to nicotine (Figure 5E PI, Cliff's delta = −0.502, 95% CI [−0.731, −0.182], $p = 0.0014$). This is a shift

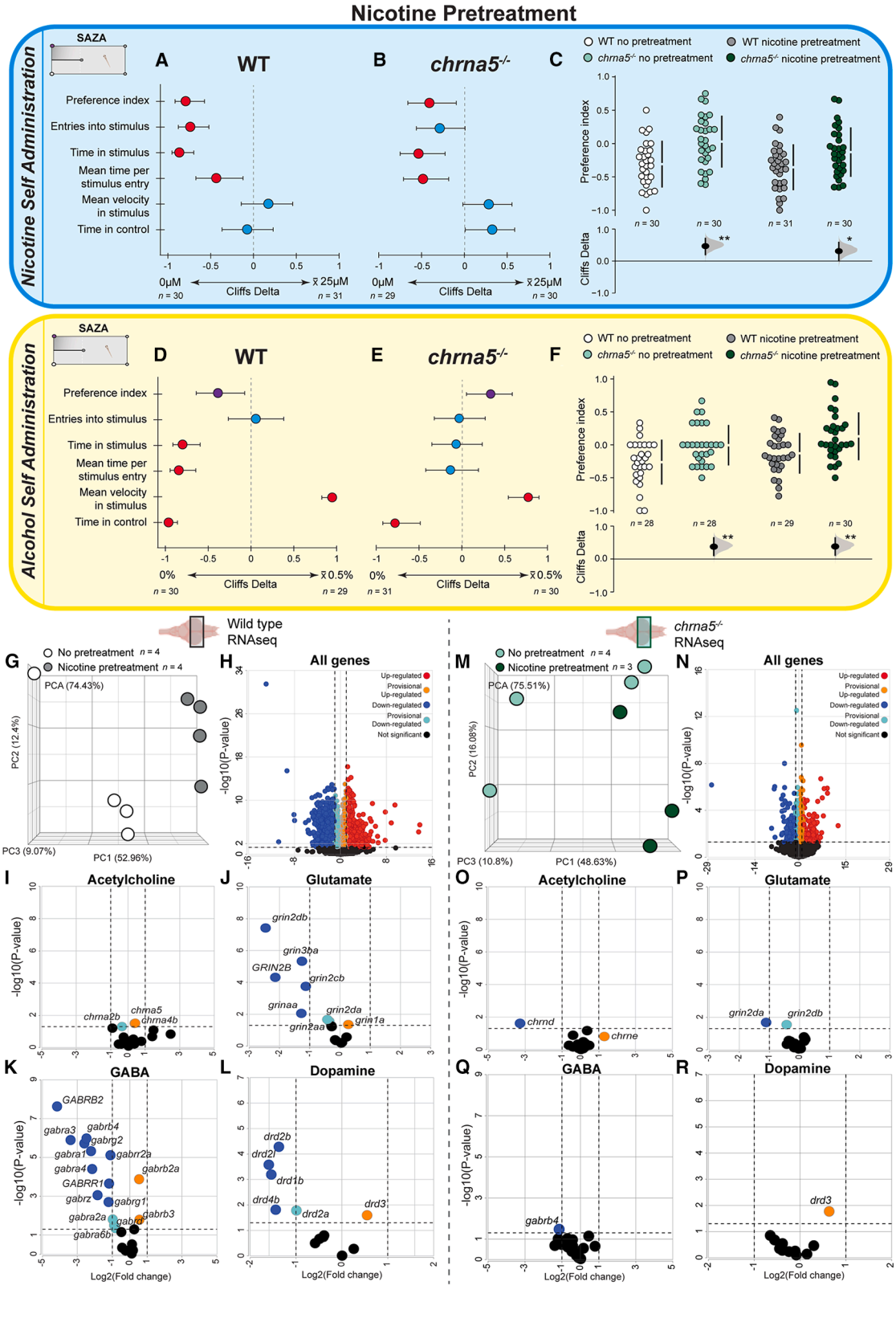

(legend on next page)

away from the neutral response observed in untreated, naive mutants (Figure 2K). This increase in aversive behaviors in both genotypes resulted in a narrowing of phenotypic differences originally seen, as the PI difference was no longer significant (Figure 5F mutant vs. WT pre-treated, Cliff's delta = 0.260, 95% CI [−0.0603, 0.527], $p = 0.0974$). Overall, these results suggested that alcohol pre-treatment shifted the nicotine response leftwards, such that the aversion in WT continued to stay pronounced, and the PI shifted from neutral to negative for mutants.

Alcohol pre-treatment changed the transcriptional profile of WT, but not *chrna5* mutants

RNA sequencing of the juvenile brains of the alcohol pre-treated fish revealed a phenomenon parallel to that observed after nicotine pre-treatment. The pre-treated and untreated samples of each genotype were separated by PCA (Figures 5G and 5M), but again, the scale of transcriptional changes in the *chrna5* mutants was fewer (Figures 5H and 5N). Curiously, the pattern of expression changes among the neurotransmitter systems was inverse to the observations after nicotine pre-treatment. Alcohol pre-treatment resulted in an upregulation of many nAChRs (Figure 5I), but little change was observed in the glutamate, GABA, and dopamine receptors that were downregulated after nicotine pre-treatment. Once again, *chrna5* mutants exhibited fewer alterations to the transcriptomic profiles of these receptor genes (Figures 5O–5R). Thus, although pre-treatment with nicotine or alcohol had minimal changes in the self-administration behaviors of WT fish, it was accompanied with gene expression profile changes in the brain. On the other hand, the behavior of the mutant *chrna5* fish was altered with limited changes in transcriptional profiles, suggesting that absence of a functional *chrna5* interfered with substance exposure induced adaptive changes in brain gene expression.

chrna5 dysfunction does not alter anxiety-like behavior in zebrafish

While the association of variants in the *CHRNA5-CHRNA3-CHRNB4* gene cluster, particularly in *CHRNA5* with nicotine and alcohol dependence have been reported extensively across numerous populations,[17,23,24,55–58] a variety of conditions frequently comorbid with nicotine dependence, including increased anxiety, alteration in attention, and appetite dysregulation are also proposed to be impacted by *CHRNA5* function.[21,27,59,60] Given that *chrna5* mutant zebrafish exhibited a phenotype of blunted aversion toward nicotine and alcohol, we evaluated if the mutation also impacted other behavioral phenotypes in fish relevant to these conditions.

To determine if *chrna5* mutant zebrafish exhibit anxiety-like behavior dissimilar to WT, we used a light/dark assay.[61] Zebrafish larvae naturally exhibit scotophobia, or dark-avoidance behaviors, at an early age. More time in the dark, entering quickly, or more frequently are indicators of reduced anxiety-like behavior in this assay.[61,62] We used up to 14 dpf larvae when they are still scotophobic and quantified the behavior of individuals following a 10 min acclimation period. The entire chamber was equally illuminated during acclimation, with half the chamber, chosen randomly, darkened in the experimental phase (Figure 6A). Both WT and mutant fish spent more time in the illuminated areas and entered the darkened area only after a few minutes. In all of these measures, however, no significant difference was observable between the WT and *chrna5* mutants (Figures 6B–6D and S14). Thus, *chrna5* had little impact on this type of anxiety-like measure in fish.

chrna5 mutants have reduced visual startle in the day, increased acoustic startle at night, and low nocturnal activity

Nicotine use and disruption of sleep have been bidirectionally linked in animal models, and the effect has been correlated to genetic variations in human studies.[63–66] Although the cholinergic system's role in sleep-wake cycle and circadian rhythms is known,[67] *chrna5*'s role has only been assessed in the context of attention.[60] To examine these behaviors and circadian phases, we tracked the activity of 7–10 dpf larval zebrafish, over 24 h, starting in the afternoon (Figure 6E). 7–10 dpf larvae swim freely in 48 well plates, facilitating high throughput assays to capture small effects associated with maintaining circadian rhythms. The assay conditions matched the 14/10 h day-night periodicity normally maintained in the facility that the larvae were entrained to. In addition, a few perturbations were introduced to examine responsivity. Light-dark-light transition periods were generated from early evening to night by alternating

Figure 4. Nicotine pre-treatment altered *chrna5* mutant acute behavioral responses to nicotine and alcohol, and effected transcriptomic changes in WT fish

(A–F) Measures of fish behavior in SAZA following a seven day nicotine pre-treatment scheme when self-administering (A–C) x̄25 μM nicotine or (D–F) x̄0.5% alcohol. Comparisons of multiple measures in (A and D) WT or (B and E) *chrna5* mutants to baseline, or (C and F) to each other by preference index, are displayed as forest plots, or Gardner-Altman and Cumming estimation plots, respectively. In the forest plots (A–E), positive values (to the right, +1) indicate a greater response in the treated condition, negative values (to the left, −1) indicate a greater response in the untreated condition, and values closer to the center (0), show equal responses between the two conditions. Data represented as Cliff's delta (±95% CI). In the Gardner-Altman plots (C and F), positive values (toward +1) indicate relative preference for the stimulus, negative values (toward −1) indicate relative preference for the control, and 0 indicates neutrality, with no relative preference for stimulus or control. Data represented as preference index (± standard deviation). Asterisks (C and F), or color (A, B, D, and E) indicate a significant difference:/blue = $p > 0.05$ (no significant difference), */purple = $p < 0.05$ and Cliff's delta > ± 0.2 & < ± 0.4 (provisional difference), **/red = $p < 0.01$ and Cliff's delta > ± 0.4 (meaningful difference). See Table S13 for the precise effect sizes and p values, corrected for multiple comparisons between genotypes against WT (C and F). Fish numbers as follows: WT/*chrna5*$^{-/-}$ nicotine-pretreated, x̄25 μM nicotine SAZA, $n = 31/30$; WT/*chrna5*$^{-/-}$ nicotine-pretreated, x̄0.5% alcohol SAZA, $n = 29/30$; WT/*chrna5*$^{-/-}$ 0 μM SAZA, $n = 30/29$; WT/*chrna5*$^{-/-}$ 0% SAZA, $n = 30/31$.

(G–R) RNA sequencing data of untreated/nicotine pretreated (G–L) WT ($n = 4/4$) and (M–R) *chrna5* mutant ($n = 4/3$) fish brain tissues, with the olfactory bulb, telencephalon and hindbrain removed, comparing untreated samples to those collected following a seven day nicotine pre-treatment scheme. (G and M) PCA separation of samples. (H–L, N–R) Volcano plots of (H and N) all genes, (I and O) nicotinic acetylcholine receptors (chrn), (J and P) glutamate receptors (grin), (K and Q) GABA receptors (gabr), (L and R) dopamine receptors (drd). Significance was categorized as adj $p > 0.05$ = non-significant (black), adj $p < 0.05$, $\log_2$ fold change 0 - ±1 = provisional up (+, orange) or down (−, cyan) regulation, adj $p < 0.05$, $\log_2$ fold change ±1–>±2 = up (+, red) or down (−, blue) regulation.

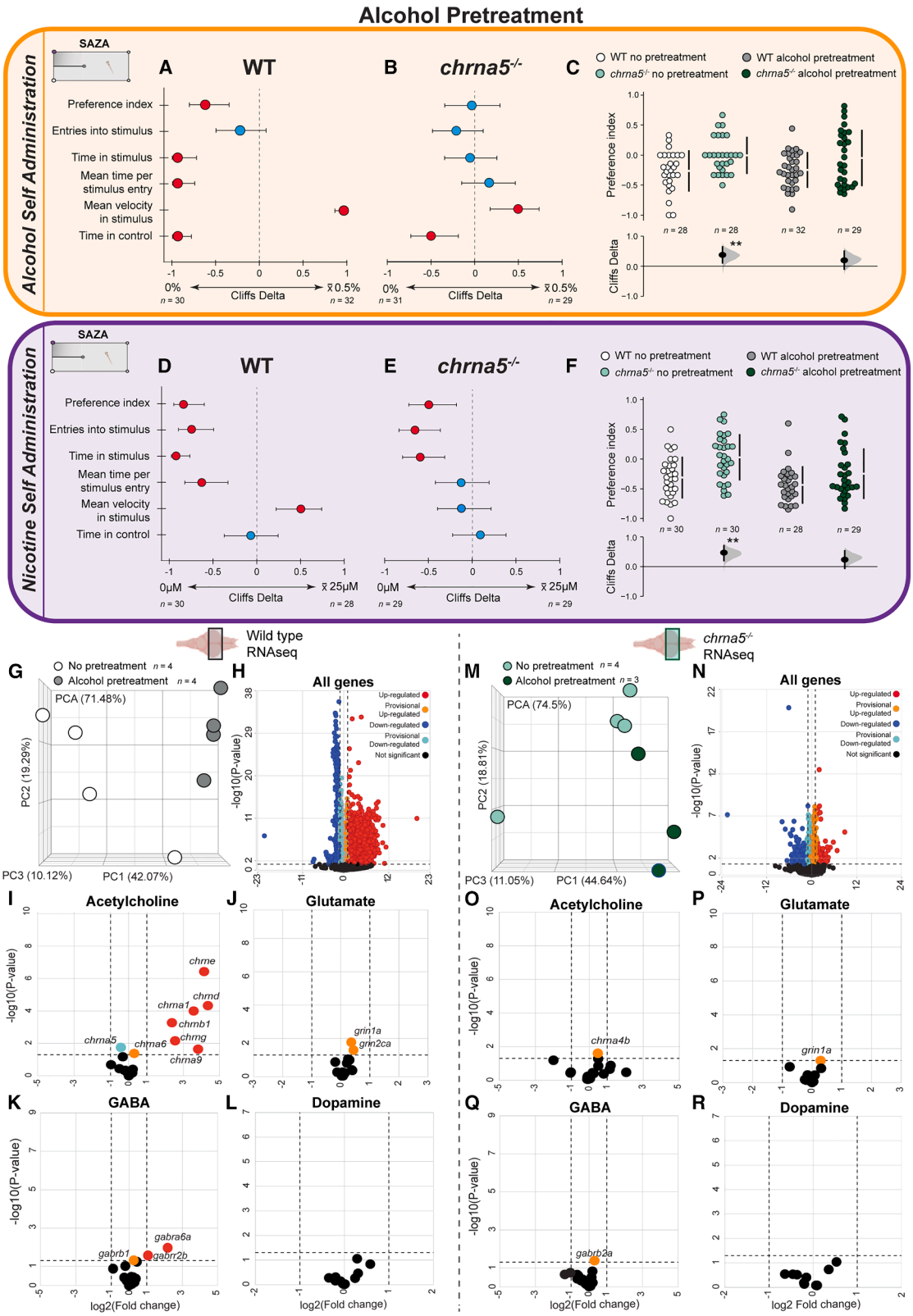

(legend on next page)

illumination blocks every 30 min to detect "dark flash" and "light flash" responses (Figure 6E).[68,69] Additionally, a few minutes of vibrational stimuli ascending and descending in intensity from night until morning were administered every hour to challenge the animals and record their response to mechanical disturbance (Figure 6E).[70] Both the WT and *chrna5* mutants maintained normal diurnal circadian rhythms, exhibiting lowest activity at night (Figure 6F Cliff's delta = 0.514, 95% CI [0.284, 0.690], $p < 0.001$, Figure 6G Cliff's delta = 0.840, 95% CI [0.699, 0.922], $p < 0.001$) and highest in the morning (Figure 6F Cliff's delta = −0.797, 95% CI [−0.894, −0.635], $p < 0.001$), Figure 6G Cliff's delta = −0.703, 95% CI [−0.834, −0.514], $p < 0.001$. However, the mutant fish displayed lower overall activity during each time period, with the greatest difference between the genotypes occurring in the night (Figure 6H Cliff's delta = 0.593, 95% CI [0.370, 0.740], $p < 0.001$). Conversely, *chrna5* mutants exhibited greater motility when startled at night, suggesting increased sensitivity to physical disturbance (Figure 6I). During the global illumination change period of the assay, both genotypes responded to both the "dark flash" (light to dark), and the "light flash" (dark to light) transitions. However, the WT fish response to the "dark flash" peaked higher than the mutants and maintained marginally greater activity until the light was switched back on (Figures 6J and 6K). In response to the "light flash", the WT again showed a slightly stronger, but non-significant, locomotor response than the mutants (Figures 6J and 6L).

chrna5 mutants consumed more protein and *Paramecia* feeds, but less egg yolk

The link between nicotine consumption and feeding behavior is well documented, with nicotine administration being associated with reduced body weight and a decrease in consumption of calorie rich foods.[71,72] Nicotine is thought to alter both the balance of orexigenic and anorexigenic peptides to change homeostatic feeding, while also exerting influence over dopamine release, which modulates hedonistic feeding behaviors.[73] In addition, genetic variance also comes into play as *CHRNA5-CHRNA3-CHRNB4* genes are expressed in the arcuate nucleus of the hypothalamus, a brain region known to impact appetite directly.[74] Global *Chrna5* receptor knockout in rodents changes preference for some food rewards, but not all.[75] To evaluate this relationship further, we examined the consumption of three types of food: a fat rich chicken egg yolk, a customized protein-rich feed, and live *Paramecium caudatum*, a natural prey item of larval zebrafish in an appetite assay.[39] The assay quantified feeding following a 2 h starvation period by fluorescent labeling of the feed, and subsequent quantification of the fluorescent signal from the gut following the feeding period (Figure 6M). Larval zebrafish, 7–10 dpf, were used to assess appetite as the gut transparency at this developmental stage allows for high throughput quantification of fluorescent feed consumed, facilitating the detection of small effect size behavioral changes. Swarm plots of the quantity of feed consumed by zebrafish across 10 batches for each food type revealed small effects on appetite for all three food types. The *chrna5* mutants tended to eat less fat-rich egg yolk than the WT (Figure 6N Cliff's delta = −0.203, 95% CI [−0.109, −0.296], $p < 0.001$), but, more protein-rich diet (Figure 6O Cliff's delta = 0.312, 95% CI [0.218, 0.404], $p < 0.001$) and *Paramecium* (Figure 6P Cliff's delta = 0.18, 95% CI [0.088, 0.274], $p = < 0.001$). Therefore, similar to the observations in rodents, *chrna5* mutants show an increased appetite for palatable food reward; however, the small, food type-dependent effects suggest that the mutation has a minor role in appetite control. Overall, the behavior of *chrna5* mutants differed from the WT in some phenotypes associated with human disorders often comorbid with substance dependence, such as appetite and circadian regulation.

DISCUSSION

Here, we generated a global *chrna5* zebrafish mutant to study the neurobehavioural consequences of dysfunction in *chrna5*, a genetic factor associated with nicotine and alcohol dependence, in addition to several frequently comorbid human disorders. *chrna5* mutants exhibited reduced aversion to acute nicotine self-administration, a phenotype also observed in loss-of-function rodents.[19,22] This suggests that dysfunctional *chrna5* impacts aversive responses to nicotine across vertebrates, and may similarly affect humans with reduced *CHRNA5* function. Notably, polymorphisms in *CHRNA5* have been associated with AUD risk independent of nicotine dependence.[23]

Figure 5. Alcohol pre-treatment abolished *chrna5* mutant phenotype of reduced aversion to nicotine, and stimulated upregulation of WT nicotinic acetylcholine receptor genes

(A–F). Measures of fish behavior in SAZA following a seven day alcohol pre-treatment scheme when self-administering (A–C) x̄0.5% alcohol or (D–F) x̄25 μM nicotine. Comparisons of multiple measures in (A and D) WT or (B and E) *chrna5* mutants to baseline, or (C and F) to each other by preference index, are displayed as forest plots, or Gardner-Altman and Cumming estimation plots, respectively. In the forest plots (A, B, D, and E), positive values (to the right, +1) indicate a greater response in the treated condition, negative values (to the left, −1) indicate a greater response in the untreated condition, and values closer to the center (0), show equal responses between the two conditions. Data represented as Cliff's delta (±95% CI). In the Gardner-Altman plots (C and F), positive values (toward +1) indicate relative preference for the stimulus, negative values (toward −1) indicate relative preference for the control, and 0 indicates neutrality, with no relative preference for stimulus or control. Data represented as preference index (± standard deviation). Asterisks (C and F), or color (A, B, D, and E) indicate a significant difference: /blue = $p > 0.05$ (no significant difference), */purple = $p < 0.05$ and Cliff's delta > ± 0.2 & < ± 0.4 (provisional difference), **/red = $p < 0.01$ and Cliff's delta > ± 0.4 (meaningful difference). See Table S14 for the precise effect sizes and p values, corrected for multiple comparisons between genotypes against WT (C and F). Fish numbers as follows: WT/*chrna5*$^{-/-}$ alcohol-pretreated, x̄0.5% alcohol SAZA, $n = 32/29$; WT/*chrna5*$^{-/-}$ alcohol-pretreated, x̄25 μM nicotine SAZA, $n = 28/29$; WT/*chrna5*$^{-/-}$ 0% SAZA, $n = 30/31$; WT/*chrna5*$^{-/-}$ 0 μM SAZA, $n = 30/29$.

(G–R) RNA sequencing data of untreated/alcohol pretreated (G–L) WT ($n = 4/4$) and (M–R) *chrna5* mutant ($n = 4/3$) fish brain tissues, with the olfactory bulb, telencephalon and hindbrain removed, comparing untreated samples to those collected following a seven day alcohol pre-treatment scheme. (G and M) PCA separation of samples. (H–L, N–R) Volcano plots of (H and N) all genes, (I and O) nicotinic acetylcholine receptors (chrn), (J and P) glutamate receptors (grin), (K and Q) GABA receptors (gabr), (L and R) dopamine receptors (drd). Significance was categorized as adj $p > 0.05$ = non-significant (black), adj $p < 0.05$, $\log_2$ fold change 0 - ±1 = provisional up (+, orange) or down (-, cyan) regulation, adj $p < 0.05$, $\log_2$ fold change ±1 - >±2 = up (+, red) or down (-, blue) regulation.

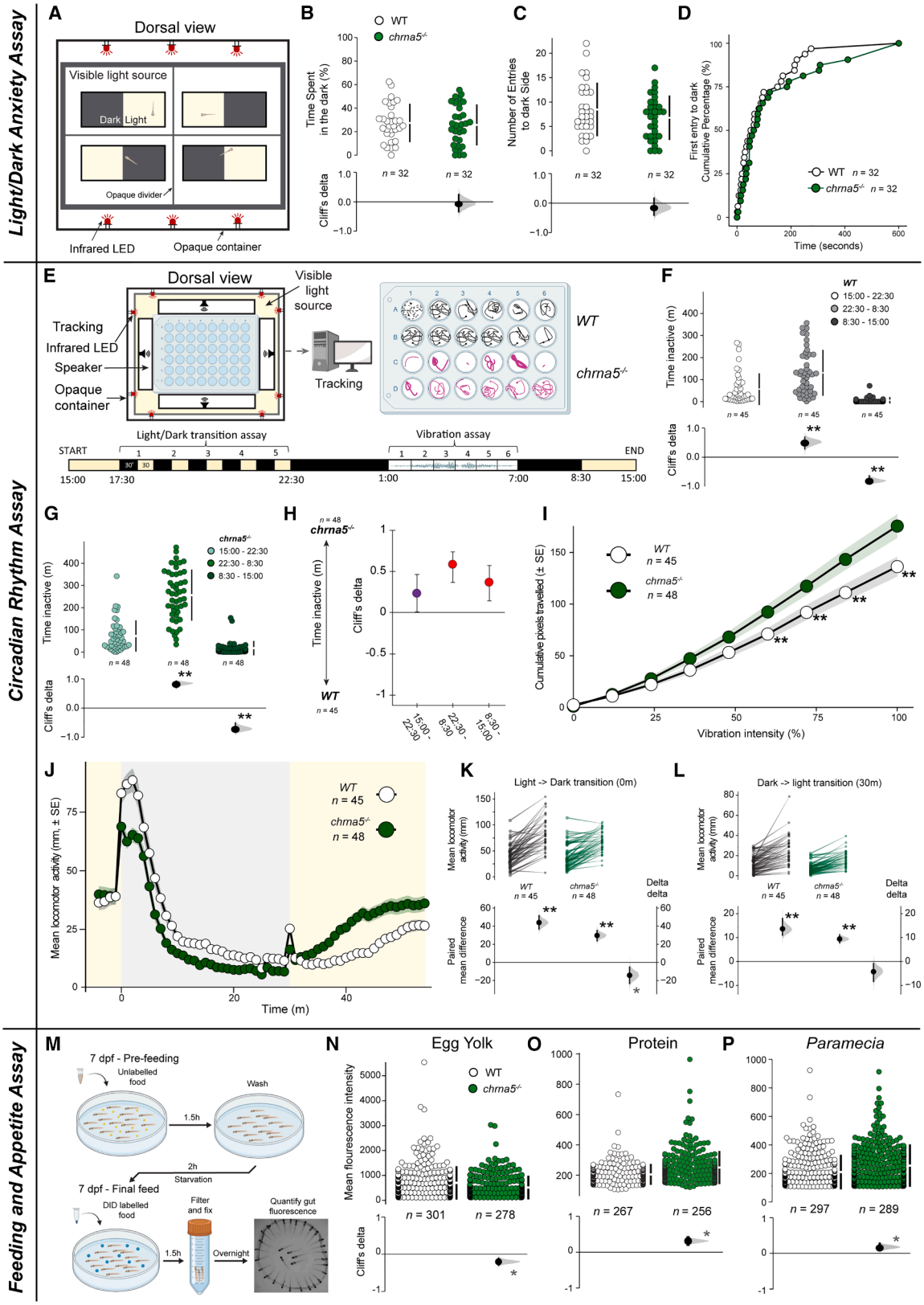

(legend on next page)

Rodent studies exploring this association have yielded mixed results, with transgenic rodents expressing human *CHRNA5* polymorphism exhibiting behaviors similar to human phenotypes,[27,76] but *Chrna5* knockout mice show an impact on alcohol consumption at certain concentrations.[25,26] In contrast, zebrafish *chrna5* mutants exhibited blunted aversion to both nicotine and alcohol self-administration. Therefore, though overlapping, the phenotype of zebrafish mutants aligns more closely with human genetic studies.

Development of substance dependence is complex and multifactorial. The dynamic changes occurring in the brain in response to repeated exposure to psychoactive substances adds an additional layer of biological complexity. Short-term exposure to nicotine over weeks can remodel reinforcement circuits that outlast drug exposure.[77] Although pre-treatments in our study lasted only a few days, both nicotine and− alcohol pre-treatments resulted in broad transcriptomic changes in the juvenile WT brains (Figures 4 and 5). The transcriptional changes observed across excitatory and inhibitory neurotransmitter systems following nicotine pre-treatment parallel findings in rodents, where modulation of dopamine receptors drd1 and drd3,[78,79] or NMDA receptors (grin) grin1–3,[80,81] reduces nicotine self-administration. Unlike our initial expectation, however, nAChR gene expression changes were minimal here (Figure 4I) with upregulation of α4 as the only exception, which may influence the dopaminergic neuronal function.[82] Thus, most molecular changes associated with even a short-term, multi-day exposure to nicotine in juvenile fish paralleled studies in mammals. That the expression of these genes showed minimal changes in *chrna5* mutants, could in turn, inform on the more prominent behavioral shifts that were absent in WT (Figure 4B).

In contrast to the transcriptional profile changes above, alcohol pre-treatment resulted in large changes in cholinergic receptor expression in the WT fish, with small or no change in the dopaminergic, GABAergic, and glutamatergic receptor gene expression. While none of the genes exhibiting altered expression have been directly linked to intake, changes were seen in non-neural genes (*chrna1*, *chrne*, *chrnd*, and *chrng*[83,84]) as well as neuronal *chrna6* and *chrna9*, both associated with nicotine[85,86] and alcohol[83,87] dependence in humans. Upregulation of GABRA6 in WT fish—consistent with human variants that reduce sedation,[88,89] may contribute to the intergenotypic velocity differences (Figure S11). In both nicotine and alcohol pre-exposure, despite limited transcriptional change, *chrna5* mutants showed strongest behavioral shifts (Figures 4 and 5), and/or increased variance (Figure 5C). Pre-treatment thus appears to trigger compensatory gene-expression in WT but not mutants, indicating an inverse link between transcriptomic change and behavioral response after pre-exposure to psychoactive substances. If this homeostatic mechanism is conserved across vertebrates, reduced *CHRNA5* function could blunt compensatory adaptation and intensify direct nicotine/alcohol effects in humans too.

Co-use of nicotine and alcohol is well documented in humans[53,54] and at a molecular level in animals,[90] making the effects of cross-treatments particularly interesting. Nicotine pre-treatment shifted both genotypes rightwards, or toward increased alcohol preference/reduced aversion (Figures 4D and 4E). On the other hand, alcohol pre-treatment shifted both genotypes leftwards or toward increased nicotine aversion (Figures 5D and 5E), implying that the drug response circuitry is not identical for nicotine and alcohol, and that receptors like drd1, drd3, and grin1-3 may contribute to a different degree depending on the substance.

Coupling whole-brain transcriptomics with behavior in the context of pre-exposure to psychoactive substances in juvenile fish, as conducted here, is also relevant for the Adolescent Brain Cognitive Development studies (ABCD[9,10,91]). Many genes exhibiting altered expression in the WT have been linked to addiction, withdrawal, and relapse in human studies, highlighting the bidirectional nature of this relationship. These included D2 and D4 receptors, which exert influence on withdrawal symptoms, place preference, and relapse to nicotine seeking behavior but not acute nicotine response,[92–94] and have human variants associated with nicotine and alcohol use.[95,96] Interestingly, D4 was also differentially expressed prior to pre-treatments (Figures S15 and S16), while D3 (drd3) known to affect alcohol consumption in rodents,[97] was one of the few genes with expression altered to a similar degree in both genotypes by nicotine pre-treatment. Additionally, *GABRA2* and *GABRA4* have several

Figure 6. Appetite and circadian rhythm disorder associated phenotypes were altered in *chrna5* mutants

(A–D) Anxiety-like behavior of 12–14 dpf larvae in light/dark assay. (A) Schematic of the light/dark assay equipment. Chambers were illuminated from below, divided into equal light and dark halves, and movement between the areas was tracked.

(B–D) Behavioral measures of (B) time spent in dark (± standard deviation [SD]), (C) number of entries to dark (±SD), and (D) cumulative first entry time of the population to the dark over the assay duration between WT (n = 32) and *chrna5* mutant (n = 32) fish.

(E–L) Circadian rhythm, vibration sensitivity, and light-dark transition behaviors of WT (n = 45) and *chrna5* mutant (n = 48) 7–10 dpf fish. Data represented as Cliff's delta (±95% CI) (E) Schematic of the circadian assay equipment and tracking (upper), and the assay timeline (lower). Yellow indicates visible lights are on, while black is off.

(F–H) Time inactive over assay duration, divided according to light on/off times in (F) WT (±SD), (G) *chrna5* mutants (±SD), and (H), between genotypes (±95% CI).

(I) Mean cumulative distance traveled by WT (n = 45) and *chrna5* mutant (n = 48) fish per vibration stimulus intensity over 6 cycles (±95% CI). Light-dark-light transition locomotor response (J) Mean locomotor activity of WT (n = 45) and *chrna5* mutant (n = 48) fish over 5 cycles (±95% CI). Yellow/gray areas indicate visible light on and off, respectively.

(K and L) Difference in individual locomotor activity within and between genotypes (delta-delta) from before and after (K) light to dark transition at 0 min, and (L) dark to light transition at 30 min.

(M–P) Feeding behavior of 7-dpf fish given assorted food types. (M) Schematic detailing feeding protocol, pre-feeding, and starvation periods prior to the labeled feed. Data represented as Cliff's delta (±95% CI) (N–P) mean fluorescent intensity gut intensity (±SD) of WT/*chrna5* mutant fish when fed (N) egg yolk (n = 301/278), (O) protein (n = 267/256), and (P) *Paramecia* (n = 297/289). * = $p < 0.05$ and Cliff's delta from ±0.2 to ±0.4 (where applicable), ** = $p < 0.01$ and Cliff's delta from > ±0.4 (where applicable). See Tables 15 and S16 for the precise effect sizes and p values, corrected for multiple comparisons within genotype between time points against 15:00–22:00 (D and G). See also Figure S14.

Table 1. Primers for single-guide RNA template

Gene	Label	Primer 5′ → 3′
chrna5	CRISPR Forward	AATTAATACGACTCACTATAGG**GTAGCGAGGAGAAGG** GTTTTAGAGCTAGAAATAG
Universal Primer	CRISPR Reverse	TTTTGCACCGACTCGGTGCCACTTTTTCAAGTTGATAA CGGACTAGCCTTATTTTAACTTGCTATTTCTAGCTCTAAAAC

Guide RNA used to generate *chrna5* CRISPR mutants. CRISPR targets are in bold.

nicotine dependence associated SNPs,[98] while *GABRR1* and *GABRR2* SNPs have been associated with alcohol dependence.[99] Finally, *GRIN2A* is associated with heroin addiction in GWAS.[100] While our study is inadequate to assess how these genes influenced the acute drug responses documented in SAZA, the transcriptional changes inform on the potential vulnerability differences in individuals with *chrna5* polymorphisms. These observations suggest that zebrafish can provide new insights into understanding the initial phases of substance use in juvenile brains.

The importance of *CHRNA5-CHRNA3-CHRNB4* gene cluster function in the habeula-IPN circuit to modulate aversion to nicotine intake has been established through several lines of evidence in rodent studies.[19,29] We therefore probed for changes in the gene expression profiles of habenula neurons in *chrna5* mutants, as the aversive responses to nicotine in fish were also altered. No overt changes could be seen (Figures 1D, S4, and S5). However, additional studies that can examine neural activity in the mutants will be necessary to establish if neuronal function changes occur.

Importantly, *CHRNA5* variants are also proposed to modulate neurons in several brain regions including the VTA dopaminergic neurons during nicotine reward and reinforcement.[101] The results of self-administration, cross-administration, anxiety, circadian rhythm, and appetite presented here may thus be suitable for whole organism level studies that mimic whole-body dysfunctional *CHRNA5*.

Mutations in *CHRNA5* are associated with vulnerability to anxiety, albeit only under certain conditions.[59,76] Mutant zebrafish displayed no altered anxiety phenotype in the light/dark assay (Figures 6B–6D), in contrast to rodent studies.[76] *CHRNA5*'s role in nicotine use disorders may thus develop independently of an anxiety phenotype. As anxiety phenotypes can vary in their manifestations and differ between social and asocial settings, additional studies examining other anxiogenic conditions will be needed to further evaluate if the dissociation manifests in other contexts.

The link between nicotine consumption and circadian rhythms is well known, while more recent investigations are beginning to uncover the bidirectional influence of genetic variation on both.[65] The differences in the activity cycle of the *chrna5* mutants especially at night (Figures 6F–6H) suggests a potential role for *chrna5* in sleep quality, independently of nicotine or alcohol consumption. Additionally, the weaker visuomotor startle response to dark flashes, but higher sensitivity to vibrational startle in the *chrna5* mutants is an interesting dissociation of the sensorimotor responses.[70] The escape responses in zebrafish larvae engage different circuits even when triggered through the same sensory modality.[102] In agreement with the *chrna5* expression reported here, a recent study using a fluorescently tagged *chrna5* expression line showed that the expression of *chrna5* is broad, in tectal neurons, hindbrain neurons, preoptic, hypothalamic, and pineal and locomotor networks.[49] As these neurons are components of the circuits engaged in visuomotor and acoustic startle,[103–105] dysfunctional *chrna5* may impact both. Further studies will be needed to evaluate if *chrna5* function is also relevant in the distributed learning circuits associated with dark flash habituation.[68]

Finally, nAChR receptors have been previously implicated in the control of feeding and appetite.[74,106] Our results suggest that *chrna5* exerts some influence over appetite, independent of nicotine administration, as evidenced by the altered consumption by mutants (Figures 6N–6P). However, the direction of change was dependent on food type—mutants consumed less egg yolk, but more of a protein-rich diet, and *Paramecium caudata*. Among these, paramecia require prey hunting behavior and coordinated locomotion, making it more challenging compared to passive feed like protein-rich and egg yolk powder.[107] Notably, reduced locomotion seen in the circadian rhythm assay (Figure 6H) did not impact the *chrna5* mutants to outperform WT larvae in hunting. As the effect sizes were small in these assays, *chrna5* may contribute only minimally to appetite regulation, and it remains to be determined if this contribution is consistent across developmental stages. This is in line with findings in rodents, that though present, *Chrna5*-containing nAChR are among the lowest abundance in hypothalamic arcuate nucleus.[106] Since these feed types differ dramatically in form, nutritional quality, and motility, further studies are necessary to understand which among macronutrient content, visual cues, or hunting drives mutant behavior.[108]

Overall, this whole-body *chrna5* mutant zebrafish exhibits aligned phenotypes with human conditions, making it a valuable and practical model for investigating the neurobiological basis of the development of SUD. Short term pre-exposure to multiple substances revealed cross-substance effects on nicotine and alcohol self-administration in these mutants, highlighting the impact of prior substance exposure on subsequent drug use behavior. Parallel transcriptomics showed altered expression of human dependence associated genes in WT fish that were absent in mutants, suggesting a disruption to homeostatic responses. Thus, our results suggest that disruption of *chrna5* potentially increases susceptibility to substance dependence via reduced drug avoidance, impairs adaptive responses, and affects behaviors such as appetite and circadian rhythms, which are frequently altered in humans in the context of SUD.

Table 2. Primers used for qPCR of *chrna5*, *chrnb4*, *chrna3*, and housekeeping genes, *actb1*, *efla*

Gene Accession #	Gene symbol	Primer 5′ → 3′
β-actin1 NM_131031.2	*actb1*	(F) AGATGACACAGATCATGTTCGAGA (R) CCAGTAGTACGACCAGAAGCG
Elongation factor I-alpha FJ915061.1	*ef1a*	(F) CTGGAGGCCAGCTCAAACAT (R) ATCAAGAAGAGTAGTACCGCTAGCATT
Alpha-5 nicotinic acetylcholine receptor ENSDARG00000003420	*chrna5*	(F) ATGGTAACAGCTCTCAGCTTGGT (R) TTAGCTAGTAATTTCAGCATAGC
Beta-4 nicotinic acetylcholine receptor ENSARG00000101677	*chrnb4*	(F) TCCTGTGTGTGTGTATGTGAATG (R) TCACATGCCGTCCCGTCTG
Alpha-3 nicotinic acetylcholine receptor ENSDARG00000100991.2	*chrna3*	(F) CCTCCTGTGTCCGACTGAAC (R) CTTCCAGTCATCCTGGACCTC

Limitations of the study

Our use of bulk RNA-sequencing on dissected brain tissue limits spatial resolution, preventing identification of the specific brain regions driving the observed transcriptional (and behavioral) changes. The absence of neural activity measurements further constrains circuit-level inferences, particularly regarding pre-treatment with nicotine or alcohol. While we sought construct validity through behavioral assays of self-administration, anxiety-like behavior, circadian rhythms, and appetite in *chrna5* mutants, extrapolation to humans should be cautious as (1) addiction is a multifactorial condition influenced by genetic, developmental, environmental, and social factors, and (2) our experiments in juvenile or younger (<14 dpf) fish may capture adaptive developmental processes that change with maturation, potentially differing from adults at steady state.

RESOURCE AVAILABILITY

Lead contact

Requests for further information and resources should be directed to, and will be fulfilled by, the lead contact, Ajay S. Mathuru (ajay.mathuru@nus.edu.sg).

Materials availability

No new unique reagents were generated as part of this study. Zebrafish mutant lines reported in the publication are available from the lead contact upon request.

Data and code availability

Raw sequencing file datasets have been deposited at Genome Sequence Archive (Genomics, Proteomics & Bioinformatics 2025) in National Genomics Data Center (Nucleic Acids Res 2025), China National Center for Bioinformation/Beijing Institute of Genomics, Chinese Academy of Sciences as (GSA: CRA032492) and are publicly available as of 2025-12-19. All original code has also been deposited in GitHub (GitHub: https://github.com/mechunderlyingbehavior/SAZA_2023; https://github.com/CarolineWeeLab/EZgut). The datasets used to generate the figures are included within the article and its supplemental files or were deposited in Mendeley Data (Mendeley Data: https://doi.org/10.17632/y3nzn8pdmj.2). Please find the public access links to all the above in the key resources table. Additional data are available from the lead contact upon request.

ACKNOWLEDGMENTS

This research was supported by the Ministry of Education (MOE), Singapore (through grant number T2EP30220-0020), Yale-NUS College (through grant numbers IG16-LR003, IG18-SG103, IG19-BG106, and SUG), and the National University of Singapore Yong Loo Lin School of Medicine Dean's Office (through grant number NUHSRO/2025/031/NUSMed/003/LOA), and by the National University of Singapore Institute of Digital Medicine (through grant number WisDM/Seed/003/2025) to ASM. We would also like to thank the Zebrafish Fish Facility (ZFF) staff at the IMCB, A*STAR for their assistance with fish husbandry; Drs. Ruey Kuang-Cheng and Caroline Wee for assistance with conducting circadian rhythm and appetite regulation assays; Li Xinrui for generating customized Python analysis scripts.

AUTHOR CONTRIBUTIONS

Conceptualization, A.S.M., T.G., and J.R.; methodology, T.G., C.K., T.D.B., J.R., and J.W.C.; formal analysis, T.G. and J.R.; investigation, T.G., J.R., and C.K.; resources, A.S.M.; writing – original draft, T.G. and J.R; writing – editing and revised, A.S.M.; writing – review, all; visualization, T.G. and J.R.; supervision, A.S.M.; project administration, A.S.M.; funding acquisition, A.S.M.

DECLARATION OF INTERESTS

The authors declare no competing interests.

DECLARATION OF GENERATIVE AI AND AI-ASSISTED TECHNOLOGIES IN THE WRITING PROCESS

During the preparation of this work, the authors used Grammarly and Gemini to assist with grammar and consistency of phrasing. After using this tool/service, the authors reviewed and edited the content as needed and take full responsibility for the content of the publication.

STAR★METHODS

Detailed methods are provided in the online version of this paper and include the following:

- KEY RESOURCES TABLE
- EXPERIMENTAL MODEL AND STUDY PARTICIPANT DETAILS
  - Fish husbandry
  - Generation of *chrna5* mutant zebrafish
- METHOD DETAILS
  - Self-administration for zebrafish assay (SAZA) apparatus setup
  - SAZA
  - Body alcohol/cotinine quantification
  - RNA extraction
  - qRT-PCR
  - Hybridisation chain reaction, RNA-fluorescent in-situ hybridisation (HCR™ RNA-FISH)
  - Protein extraction
  - Western blot

SUPPLEMENTAL INFORMATION

Supplemental information can be found online at https://doi.org/10.1016/j.isci.2026.114735.

Received: July 24, 2025
Revised: November 9, 2025
Accepted: January 14, 2026
Published: January 19, 2026

REFERENCES

1. Rehm, J., and Shield, K.D. (2019). Global Burden of Disease and the Impact of Mental and Addictive Disorders. Curr. Psychiatry Rep. *21*, 10.
2. Wang, M., and Yu, T. (2025). Global burden of disease among adolescents and young adults with drug use disorders, 1990-2021: based on GBD 2021. Front. Public Health *13*, 1583812.
3. Liu, Y., Zhang, N., Ren, W., Lv, X., Ran, S., Tan, X., and Zhao, Q. (2025). The evolving burden of drug use disorders: a comprehensive epidemiological analysis from the 2021 Global Burden of Disease study. Front. Psychiatry *16*, 1647269.
4. CDCTobaccoFree (2020). Fast Facts. Centers for Disease Control and Prevention. https://www.cdc.gov/tobacco/data_statistics/fact_sheets/fast_facts/index.htm.
5. GBD 2019 Tobacco Collaborators (2021). Spatial, temporal, and demographic patterns in prevalence of smoking tobacco use and attributable disease burden in 204 countries and territories, 1990-2019: a systematic analysis from the Global Burden of Disease Study 2019. Lancet *397*, 2337–2360.
6. Larsson, S.C., and Burgess, S. (2022). Appraising the causal role of smoking in multiple diseases: A systematic review and meta-analysis of Mendelian randomization studies. EBioMedicine *82*, 104154.
7. Li, M.D., and Burmeister, M. (2009). New insights into the genetics of addiction. Nat. Rev. Genet. *10*, 225–231.
8. Volkow, N.D., and Blanco, C. (2023). Substance use disorders: a comprehensive update of classification, epidemiology, neurobiology, clinical aspects, treatment and prevention. World Psychiatry *22*, 203–229.
9. Miller, A.P., Baranger, D.A.A., Paul, S.E., Garavan, H., Mackey, S., Tapert, S.F., LeBlanc, K.H., Agrawal, A., and Bogdan, R. (2024). Neuroanatomical Variability and Substance Use Initiation in Late Childhood and Early Adolescence. JAMA Netw. Open *7*, e2452027.
10. Pichardo, F., and Wilson, S. (2024). The Adolescent Brain Cognitive Development Study and How We Think About Addiction. JAMA Netw. Open *7*, e2451997.
11. Picciotto, M.R., and Kenny, P.J. (2021). Mechanisms of Nicotine Addiction. Cold Spring Harb. Perspect. Med. *11*, a039610. https://doi.org/10.1101/cshperspect.a039610.
12. Thorgeirsson, T.E., Geller, F., Sulem, P., Rafnar, T., Wiste, A., Magnusson, K.P., Manolescu, A., Thorleifsson, G., Stefansson, H., Ingason, A., et al. (2008). A variant associated with nicotine dependence, lung cancer and peripheral arterial disease. Nature *452*, 638–642.
13. Spitz, M.R., Amos, C.I., Dong, Q., Lin, J., and Wu, X. (2008). The CHRNA5-A3 region on chromosome 15q24-25.1 is a risk factor both for nicotine dependence and for lung cancer. J. Natl. Cancer Inst. *100*, 1552–1556.
14. Jensen, K.P., DeVito, E.E., Herman, A.I., Valentine, G.W., Gelernter, J., and Sofuoglu, M. (2015). A CHRNA5 Smoking Risk Variant Decreases the Aversive Effects of Nicotine in Humans. Neuropsychopharmacology *40*, 2813–2821.
15. Icick, R., Forget, B., Cloëz-Tayarani, I., Pons, S., Maskos, U., and Besson, M. (2020). Genetic susceptibility to nicotine addiction: Advances and shortcomings in our understanding of the CHRNA5/A3/B4 gene cluster contribution. Neuropharmacology *177*, 108234.
16. Lee, S.-H., Ahn, W.-Y., Seweryn, M., and Sadee, W. (2018). Combined genetic influence of the nicotinic receptor gene cluster CHRNA5/A3/B4 on nicotine dependence. BMC Genom. *19*, 826.
17. Ware, J.J., van den Bree, M., and Munafò, M.R. (2012). From Men to Mice: CHRNA5/CHRNA3, Smoking Behavior and Disease. Nicotine Tob. Res. *14*, 1291–1299. https://doi.org/10.1093/ntr/nts106.
18. Morton, G., Nasirova, N., Sparks, D.W., Brodsky, M., Sivakumaran, S., Lambe, E.K., and Turner, E.E. (2018). Chrna5-Expressing Neurons in the Interpeduncular Nucleus Mediate Aversion Primed by Prior Stimulation or Nicotine Exposure. J. Neurosci. *38*, 6900–6920.
19. Fowler, C.D., Lu, Q., Johnson, P.M., Marks, M.J., and Kenny, P.J. (2011). Habenular α5 nicotinic receptor subunit signalling controls nicotine intake. Nature *471*, 597–601.
20. Exley, R., McIntosh, J.M., Marks, M.J., Maskos, U., and Cragg, S.J. (2012). Striatal α5 nicotinic receptor subunit regulates dopamine transmission in dorsal striatum. J. Neurosci. *32*, 2352–2356.
21. Mathuru, A.S. (2018). A little rein on addiction. Semin. Cell Dev. Biol. *78*, 120–129.
22. Fowler, C.D., Tuesta, L., and Kenny, P.J. (2013). Role of α5* nicotinic acetylcholine receptors in the effects of acute and chronic nicotine treatment on brain reward function in mice. Psychopharmacology *229*, 503–513. https://doi.org/10.1007/s00213-013-3235-1.
23. Wang, J.C., Grucza, R., Cruchaga, C., Hinrichs, A.L., Bertelsen, S., Budde, J.P., Fox, L., Goldstein, E., Reyes, O., Saccone, N., et al. (2009). Genetic variation in the CHRNA5 gene affects mRNA levels and is associated with risk for alcohol dependence. Mol. Psychiatry *14*, 501–510.
24. Venkatesh, S.K., Stangl, B.L., Quijano Cardé, N.A., De Biasi, M., and Ramchandani, V.A. (2021). 36344 Effect of CHRNA5 genetic variation and smoking on alcohol related phenotypes in healthy adult drinkers. J. Clin. Transl. Sci. *5*, 2–3.
25. Dawson, A., Wolstenholme, J.T., Roni, M.A., Campbell, V.C., Jackson, A., Slater, C., Bagdas, D., Perez, E.E., Bettinger, J.C., De Biasi, M., et al. (2018). Knockout of alpha 5 nicotinic acetylcholine receptors subunit alters ethanol-mediated behavioral effects and reward in mice. Neuropharmacology *138*, 341–348.
26. Santos, N., Chatterjee, S., Henry, A., Holgate, J., and Bartlett, S.E. (2013). The α5 neuronal nicotinic acetylcholine receptor subunit plays an important role in the sedative effects of ethanol but does not modulate consumption in mice. Alcohol Clin. Exp. Res. *37*, 655–662.
27. Besson, M., Forget, B., Correia, C., Blanco, R., and Maskos, U. (2019). Profound alteration in reward processing due to a human polymorphism in CHRNA5: a role in alcohol dependence and feeding behavior. Neuropsychopharmacology *44*, 1906–1916.
28. Frie, J.A., Nolan, C.J., Murray, J.E., and Khokhar, J.Y. (2022). Addiction-Related Outcomes of Nicotine and Alcohol Co-use: New Insights Following the Rise in Vaping. Nicotine Tob. Res. *24*, 1141–1149.
29. Mondoloni, S., Nguyen, C., Vicq, E., Ciscato, M., Jehl, J., Durand-de Cuttoli, R., Torquet, N., Tolu, S., Pons, S., Maskos, U., et al. (2023). Prolonged nicotine exposure reduces aversion to the drug in mice by altering nicotinic transmission in the interpeduncular nucleus. eLife *12*, e80767. https://doi.org/10.7554/eLife.80767.
30. Gentry, C.L., and Lukas, R.J. (2002). Regulation of nicotinic acetylcholine receptor numbers and function by chronic nicotine exposure. Curr. Drug Targets: CNS Neurol. Disord. *1*, 359–385.

31. Liu, M., Guo, S., Huang, D., Hu, D., Wu, Y., Zhou, W., and Song, W. (2022). Chronic Alcohol Exposure Alters Gene Expression and Neurodegeneration Pathways in the Brain of Adult Mice. J. Alzheimers Dis. *86*, 315–331.

32. Kutlu, M.G., and Gould, T.J. (2015). Nicotine modulation of fear memories and anxiety: Implications for learning and anxiety disorders. Biochem. Pharmacol. *97*, 498–511.

33. Watanabe, S., Hofman, M.A., and Shimizu, T. (2017). Evolution of the Brain, Cognition, and Emotion in Vertebrates (Springer).

34. Wullimann, M.F., Rupp, B., and Reichert, H. (1996). Neuroanatomy of the Zebrafish Brain: A Topological Atlas (Springer).

35. von Trotha, J.W., Vernier, P., and Bally-Cuif, L. (2014). Emotions and motivated behavior converge on an amygdala-like structure in the zebrafish. Eur. J. Neurosci. *40*, 3302–3315.

36. Cully, M. (2019). Zebrafish earn their drug discovery stripes. Nat. Rev. Drug Discov. *18*, 811–813.

37. Egan, R.J., Bergner, C.L., Hart, P.C., Cachat, J.M., Canavello, P.R., Elegante, M.F., Elkhayat, S.I., Bartels, B.K., Tien, A.K., Tien, D.H., et al. (2009). Understanding behavioral and physiological phenotypes of stress and anxiety in zebrafish. Behav. Brain Res. *205*, 38–44.

38. Frøland Steindal, I.A., and Whitmore, D. (2019). Circadian Clocks in Fish-What Have We Learned so far? Biology *8*, 17. https://doi.org/10.3390/biology8010017.

39. Wee, C.L., Song, E.Y., Johnson, R.E., Ailani, D., Randlett, O., Kim, J.-Y., Nikitchenko, M., Bahl, A., Yang, C.-T., Ahrens, M.B., et al. (2019). A bidirectional network for appetite control in larval zebrafish. eLife *8*, e43775. https://doi.org/10.7554/eLife.43775.

40. Klee, E.W., Schneider, H., Clark, K.J., Cousin, M.A., Ebbert, J.O., Hooten, W.M., Karpyak, V.M., Warner, D.O., and Ekker, S.C. (2012). Zebrafish: a model for the study of addiction genetics. Hum. Genet. *131*, 977–1008.

41. Nathan, F.M., Kibat, C., Goel, T., Stewart, J., Claridge-Chang, A., and Mathuru, A.S. (2022). Contingent stimulus delivery assay for zebrafish reveals a role for CCSER1 in alcohol preference. Addict. Biol. *27*, e13126.

42. Schneider, H., Pearson, A., Harris, D., Krause, S., Tucker, A., Gardner, K., and Chinyanya, K. (2023). Identification of nicotine-seeking and avoiding larval zebrafish using a new three-choice behavioral assay. Front. Mol. Neurosci. *16*, 1112927.

43. Bossé, G.D., and Peterson, R.T. (2017). Development of an opioid self-administration assay to study drug seeking in zebrafish. Behav. Brain Res. *335*, 158–166.

44. Raine, J., Kibat, C., Banerjee, T.D., Monteiro, A., and Mathuru, A.S. (2025). Modulates Alcohol Response. J. Neurosci. *45*, e0304252025. https://doi.org/10.1523/JNEUROSCI.0304-25.2025.

45. Jumper, J., Evans, R., Pritzel, A., Green, T., Figurnov, M., Ronneberger, O., Tunyasuvunakool, K., Bates, R., Žídek, A., Potapenko, A., et al. (2021). Highly accurate protein structure prediction with AlphaFold. Nature *596*, 583–589.

46. Kunst, M., Laurell, E., Mokayes, N., Kramer, A., Kubo, F., Fernandes, A.M., Förster, D., Dal Maschio, M., and Baier, H. (2019). A Cellular-Resolution Atlas of the Larval Zebrafish Brain. Neuron *103*, 21–38.e5.

47. Hong, E., Santhakumar, K., Akitake, C.A., Ahn, S.J., Thisse, C., Thisse, B., Wyart, C., Mangin, J.-M., and Halpern, M.E. (2013). Cholinergic left-right asymmetry in the habenulo-interpeduncular pathway. Proc. Natl. Acad. Sci. USA *110*, 21171–21176.

48. Pandey, S., Shekhar, K., Regev, A., and Schier, A.F. (2018). Comprehensive Identification and Spatial Mapping of Habenular Neuronal Types Using Single-Cell RNA-Seq. Curr. Biol. *28*, 1052–1065.e7.

49. Hua, Y., Habicher, J., Carl, M., Manuel, R., and Boije, H. (2025). Novel Transgenic Zebrafish Lines to Study the CHRNA3-B4-A5 Gene Cluster. Dev. Neurobiol. *85*, e22956.

50. Banerjee, T.D., Raine, J., Mathuru, A.S., Chen, K.H., and Monteiro, A. (2025). Spatial mRNA profiling using rapid amplified multiplexed-FISH (RAM-FISH). https://doi.org/10.2139/ssrn.5133410.

51. Lockwood, B., Bjerke, S., Kobayashi, K., and Guo, S. (2004). Acute effects of alcohol on larval zebrafish: a genetic system for large-scale screening. Pharmacol. Biochem. Behav. *77*, 647–654.

52. Hahn, B., and Stolerman, I.P. (2002). Nicotine-induced attentional enhancement in rats: effects of chronic exposure to nicotine. Neuropsychopharmacology *27*, 712–722.

53. Dani, J.A., and Harris, R.A. (2005). Nicotine addiction and comorbidity with alcohol abuse and mental illness. Nat. Neurosci. *8*, 1465–1470.

54. Schlaepfer, I.R., Hoft, N.R., and Ehringer, M.A. (2008). The genetic components of alcohol and nicotine co-addiction: from genes to behavior. Curr. Drug Abuse Rev. *1*, 124–134.

55. Pandey, N., Pal, S., Sharma, L.K., Guleria, R., Mohan, A., and Srivastava, T. (2017). SNP rs16969968 as a Strong Predictor of Nicotine Dependence and Lung Cancer Risk in a North Indian Population. Asian Pac. J. Cancer Prev. *18*, 3073–3079.

56. Olfson, E., Saccone, N.L., Johnson, E.O., Chen, L.-S., Culverhouse, R., Doheny, K., Foltz, S.M., Fox, L., Gogarten, S.M., Hartz, S., et al. (2016). Rare, low frequency and common coding variants in CHRNA5 and their contribution to nicotine dependence in European and African Americans. Mol. Psychiatry *21*, 601–607.

57. Chaity, N.I., and Apu, M.N.H. (2022). rs16969968 and rs578776 polymorphisms are associated with multiple nicotine dependence phenotypes in Bangladeshi smokers. Heliyon *8*, e09947.

58. Al-Eitan, L., Shatnawi, M., and Alghamdi, M. (2024). Investigating CHRNA5, CHRNA3, and CHRNB4 variants in the genetic landscape of substance use disorder in Jordan. BMC Psychiatry *24*, 436.

59. Chen, L.-S., Xian, H., Grucza, R.A., Saccone, N.L., Wang, J.C., Johnson, E.O., Breslau, N., Hatsukami, D., and Bierut, L.J. (2012). Nicotine dependence and comorbid psychiatric disorders: examination of specific genetic variants in the CHRNA5-A3-B4 nicotinic receptor genes. Drug Alcohol Depend. *123*, S42–S51.

60. Schuch, J.B., Polina, E.R., Rovaris, D.L., Kappel, D.B., Mota, N.R., Cupertino, R.B., Silva, K.L., Guimarães-da-Silva, P.O., Karam, R.G., Salgado, C.A.I., et al. (2016). Pleiotropic effects of Chr15q25 nicotinic gene cluster and the relationship between smoking, cognition and ADHD. J. Psychiatr. Res. *80*, 73–78.

61. Jesuthasan, S., Krishnan, S., Cheng, R.-K., and Mathuru, A. (2021). Neural correlates of state transitions elicited by a chemosensory danger cue. Prog. Neuropsychopharmacol. Biol. Psychiatry *111*, 110110.

62. Bai, Y., Liu, H., Huang, B., Wagle, M., and Guo, S. (2016). Identification of environmental stressors and validation of light preference as a measure of anxiety in larval zebrafish. BMC Neurosci. *17*, 63.

63. O'Hara, B.F., Edgar, D.M., Cao, V.H., Wiler, S.W., Heller, H.C., Kilduff, T.S., and Miller, J.D. (1998). Nicotine and nicotinic receptors in the circadian system. Psychoneuroendocrinology *23*, 161–173.

64. Jaehne, A., Loessl, B., Bárkai, Z., Riemann, D., and Hornyak, M. (2009). Effects of nicotine on sleep during consumption, withdrawal and replacement therapy. Sleep Med. Rev. *13*, 363–377.

65. Gibson, M., Munafò, M.R., Taylor, A.E., and Treur, J.L. (2019). Evidence for Genetic Correlations and Bidirectional, Causal Effects Between Smoking and Sleep Behaviors. Nicotine Tob. Res. *21*, 731–738.

66. Garcia, A.N., and Salloum, I.M. (2015). Polysomnographic sleep disturbances in nicotine, caffeine, alcohol, cocaine, opioid, and cannabis use: A focused review. Am. J. Addict. *24*, 590–598.

67. Steriade, M. (2004). Acetylcholine systems and rhythmic activities during the waking–sleep cycle. Prog. Brain Res. *145*, 179–196.

68. Lamiré, L.A., Haesemeyer, M., Engert, F., Granato, M., and Randlett, O. (2023). Functional and pharmacological analyses of visual habituation learning in larval zebrafish. eLife *12*, RP84926. https://doi.org/10.7554/eLife.84926.

69. Randlett, O., Haesemeyer, M., Forkin, G., Shoenhard, H., Schier, A.F., Engert, F., and Granato, M. (2019). Distributed Plasticity Drives Visual Habituation Learning in Larval Zebrafish. Curr. Biol. *29*, 1337–1345.e4.

70. Ravan, A., Chemla, Y.R., and Gruebele, M. (2025). Larval zebrafish swim bouts in three dimensions reveal both new and redundant behaviours. J. R. Soc. Interface *22*, 20250065.

71. Grunberg, N.E. (1982). The effects of nicotine and cigarette smoking on food consumption and taste preferences. Addict. Behav. *7*, 317–331.

72. Hofstetter, A., Schutz, Y., Jéquier, E., and Wahren, J. (1986). Increased 24-hour energy expenditure in cigarette smokers. N. Engl. J. Med. *314*, 79–82.

73. Stojakovic, A., Espinosa, E.P., Farhad, O.T., and Lutfy, K. (2017). Effects of nicotine on homeostatic and hedonic components of food intake. J. Endocrinol. *235*, R13–R31.

74. Calarco, C.A., and Picciotto, M.R. (2020). Nicotinic Acetylcholine Receptor Signaling in the Hypothalamus: Mechanisms Related to Nicotine's Effects on Food Intake. Nicotine Tob. Res. *22*, 152–163.

75. Breum, A.W., Falk, S., Svendsen, C.S.A., Nicolaisen, T.S., Mathiesen, C.V., Maskos, U., and Clemmensen, C. (2022). Divergent Roles of α5 and β4 Nicotinic Receptor Subunits in Food Reward and Nicotine-induced Weight Loss in Male Mice. Endocrinology *163*, bqac079.

76. Tochon, L., Henkous, N., Besson, M., Maskos, U., and David, V. (2024). Distinct Chrna5 mutations link excessive alcohol use to types I/II vulnerability profiles and IPN GABAergic neurons. Transl. Psychiatry *14*, 461.

77. Lüscher, C., and Malenka, R.C. (2011). Drug-evoked synaptic plasticity in addiction: from molecular changes to circuit remodeling. Neuron *69*, 650–663.

78. Chellian, R., Behnood-Rod, A., Wilson, R., Lin, K., King, G.W.-Y., and Bruijnzeel, A.W. (2023). Dopamine D1-like receptor activation decreases nicotine intake in rats with short or long access to nicotine. Addict. Biol. *28*, e13312.

79. Ross, J.T., Corrigall, W.A., Heidbreder, C.A., and LeSage, M.G. (2007). Effects of the selective dopamine D3 receptor antagonist SB-277011A on the reinforcing effects of nicotine as measured by a progressive-ratio schedule in rats. Eur. J. Pharmacol. *559*, 173–179.

80. Kenny, P.J., Chartoff, E., Roberto, M., Carlezon, W.A., Jr., and Markou, A. (2009). NMDA receptors regulate nicotine-enhanced brain reward function and intravenous nicotine self-administration: role of the ventral tegmental area and central nucleus of the amygdala. Neuropsychopharmacology *34*, 266–281.

81. Blokhina, E.A., Kashkin, V.A., Zvartau, E.E., Danysz, W., and Bespalov, A.Y. (2005). Effects of nicotinic and NMDA receptor channel blockers on intravenous cocaine and nicotine self-administration in mice. Eur. Neuropsychopharmacol. *15*, 219–225.

82. Champtiaux, N., Gotti, C., Cordero-Erausquin, M., David, D.J., Przybylski, C., Léna, C., Clementi, F., Moretti, M., Rossi, F.M., Le Novère, N., et al. (2003). Subunit composition of functional nicotinic receptors in dopaminergic neurons investigated with knock-out mice. J. Neurosci. *23*, 7820–7829.

83. Zuo, L., Tan, Y., Li, C.-S.R., Wang, Z., Wang, K., Zhang, X., Lin, X., Chen, X., Zhong, C., Wang, X., et al. (2016). Associations of rare nicotinic cholinergic receptor gene variants to nicotine and alcohol dependence. Am. J. Med. Genet. B Neuropsychiatr. Genet. *171*, 1057–1071.

84. Gotti, C., Zoli, M., and Clementi, F. (2006). Brain nicotinic acetylcholine receptors: native subtypes and their relevance. Trends Pharmacol. Sci. *27*, 482–491.

85. Thorgeirsson, T.E., Gudbjartsson, D.F., Surakka, I., Vink, J.M., Amin, N., Geller, F., Sulem, P., Rafnar, T., Esko, T., Walter, S., et al. (2010). Sequence variants at CHRNB3-CHRNA6 and CYP2A6 affect smoking behavior. Nat. Genet. *42*, 448–453.

86. Yang, J., Wang, S., Yang, Z., Hodgkinson, C.A., Iarikova, P., Ma, J.Z., Payne, T.J., Goldman, D., and Li, M.D. (2015). The contribution of rare and common variants in 30 genes to risk nicotine dependence. Mol. Psychiatry *20*, 1467–1478.

87. Hoft, N.R., Corley, R.P., McQueen, M.B., Huizinga, D., Menard, S., and Ehringer, M.A. (2009). SNPs in CHRNA6 and CHRNB3 are associated with alcohol consumption in a nationally representative sample. Genes Brain Behav. *8*, 631–637.

88. García-Martín, E., Ramos, M.I., Cornejo-García, J.A., Galván, S., Perkins, J.R., Rodríguez-Santos, L., Alonso-Navarro, H., Jiménez-Jiménez, F.J., and Agúndez, J.A.G. (2018). Missense Gamma-Aminobutyric Acid Receptor Polymorphisms Are Associated with Reaction Time, Motor Time, and Ethanol Effects. Front. Cell. Neurosci. *12*, 10.

89. Cui, W.-Y., Seneviratne, C., Gu, J., and Li, M.D. (2012). Genetics of GABAergic signaling in nicotine and alcohol dependence. Hum. Genet. *131*, 843–855.

90. Doyon, W.M., Dong, Y., Ostroumov, A., Thomas, A.M., Zhang, T.A., and Dani, J.A. (2013). Nicotine decreases ethanol-induced dopamine signaling and increases self-administration via stress hormones. Neuron *79*, 530–540.

91. Choi, M., Aliev, F., Barr, P.B., Cooke, M.E., Kuo, S.I., Salvatore, J.E., Dick, D.M., and Brislin, S.J. (2025). Genetic, psychological, and environmental factors are uniquely associated with onset of alcohol use in the adolescent brain cognitive development (ABCD) study. Transl. Psychiatry *15*, 229.

92. Grieder, T.E., George, O., Tan, H., George, S.R., Le Foll, B., Laviolette, S.R., and van der Kooy, D. (2012). Phasic D1 and tonic D2 dopamine receptor signaling double dissociate the motivational effects of acute nicotine and chronic nicotine withdrawal. Proc. Natl. Acad. Sci. USA *109*, 3101–3106.

93. Wilar, G., Shinoda, Y., Sasaoka, T., and Fukunaga, K. (2019). Crucial Role of Dopamine D2 Receptor Signaling in Nicotine-Induced Conditioned Place Preference. Mol. Neurobiol. *56*, 7911–7928.

94. Yan, Y., Pushparaj, A., Le Strat, Y., Gamaleddin, I., Barnes, C., Justinova, Z., Goldberg, S.R., and Le Foll, B. (2012). Blockade of dopamine d4 receptors attenuates reinstatement of extinguished nicotine-seeking behavior in rats. Neuropsychopharmacology *37*, 685–696.

95. Connor, J.P., Young, R.M., Lawford, B.R., Saunders, J.B., Ritchie, T.L., and Noble, E.P. (2007). Heavy nicotine and alcohol use in alcohol dependence is associated with D2 dopamine receptor (DRD2) polymorphism. Addict. Behav. *32*, 310–319.

96. Luciano, M., Zhu, G., Kirk, K.M., Whitfield, J.B., Butler, R., Heath, A.C., Madden, P.A.F., and Martin, N.G. (2004). Effects of dopamine receptor D4 variation on alcohol and tobacco use and on novelty seeking: multivariate linkage and association analysis. Am. J. Med. Genet. B Neuropsychiatr. Genet. *124B*, 113–123.

97. Thanos, P.K., Katana, J.M., Ashby, C.R., Jr., Michaelides, M., Gardner, E.L., Heidbreder, C.A., and Volkow, N.D. (2005). The selective dopamine D3 receptor antagonist SB-277011-A attenuates ethanol consumption in ethanol preferring (P) and non-preferring (NP) rats. Pharmacol. Biochem. Behav. *81*, 190–197.

98. Agrawal, A., Pergadia, M.L., Saccone, S.F., Hinrichs, A.L., Lessov-Schlaggar, C.N., Saccone, N.L., Neuman, R.J., Breslau, N., Johnson, E., Hatsukami, D., et al. (2008). Gamma-aminobutyric acid receptor genes and nicotine dependence: evidence for association from a case-control study. Addiction *103*, 1027–1038.

99. Xuei, X., Flury-Wetherill, L., Dick, D., Goate, A., Tischfield, J., Nurnberger, J., Jr., Schuckit, M., Kramer, J., Kuperman, S., Hesselbrock, V., et al. (2010). GABRR1 and GABRR2, encoding the GABA-A receptor subunits rho1 and rho2, are associated with alcohol dependence. Am. J. Med. Genet. B Neuropsychiatr. Genet. *153B*, 418–427.

100. Zhao, B., Zhu, Y., Wang, W., Cui, H.-M., Wang, Y.-P., and Lai, J.-H. (2013). Analysis of variations in the glutamate receptor, N-methyl D-aspartate 2A (GRIN2A) gene reveals their relative importance as genetic susceptibility factors for heroin addiction. PLoS One *8*, e70817.

101. Yang, K., McLaughlin, I., Shaw, J.K., Quijano-Cardé, N., Dani, J.A., and De Biasi, M. (2023). CHRNA5 gene variation affects the response of VTA dopaminergic neurons during chronic nicotine exposure and withdrawal. Neuropharmacology *235*, 109547.

102. Fotowat, H., and Engert, F. (2023). Neural circuits underlying habituation of visually evoked escape behaviors in larval zebrafish. eLife *12*, e82916. https://doi.org/10.7554/eLife.82916.

103. Fernandes, A.M., Fero, K., Arrenberg, A.B., Bergeron, S.A., Driever, W., and Burgess, H.A. (2012). Deep brain photoreceptors control light-seeking behavior in zebrafish larvae. Curr. Biol. *22*, 2042–2047.

104. Wexler, Y., Huang, D., Medvetzky, A., Armbruster, D., Driever, W., Yan, J., and Gothilf, Y. (2024). Zebrafish Dark-Dependent Behavior Requires Phototransduction by the Pineal Gland. J. Pineal Res. *76*, e70021.

105. Vanwalleghem, G., Heap, L.A., and Scott, E.K. (2017). A profile of auditory-responsive neurons in the larval zebrafish brain. J. Comp. Neurol. *525*, 3031–3043.

106. Calarco, C.A., Li, Z., Taylor, S.R., Lee, S., Zhou, W., Friedman, J.M., Mineur, Y.S., Gotti, C., and Picciotto, M.R. (2018). Molecular and cellular characterization of nicotinic acetylcholine receptor subtypes in the arcuate nucleus of the mouse hypothalamus. Eur. J. Neurosci. *48*, 1600–1619. https://doi.org/10.1111/ejn.13966.

107. Bianco, I.H., Kampff, A.R., and Engert, F. (2011). Prey capture behavior evoked by simple visual stimuli in larval zebrafish. Front. Syst. Neurosci. *5*, 101.

108. Zhu, S.I., and Goodhill, G.J. (2023). From perception to behavior: The neural circuits underlying prey hunting in larval zebrafish. Front. Neural Circuits *17*, 1087993.

109. Hwang, W.Y., Fu, Y., Reyon, D., Maeder, M.L., Tsai, S.Q., Sander, J.D., Peterson, R.T., Yeh, J.-R.J., and Joung, J.K. (2013). Efficient genome editing in zebrafish using a CRISPR-Cas system. Nat. Biotechnol. *31*, 227–229.

110. Krishnan, S., Mathuru, A.S., Kibat, C., Rahman, M., Lupton, C.E., Stewart, J., Claridge-Chang, A., Yen, S.-C., and Jesuthasan, S. (2014). The Right Dorsal Habenula Limits Attraction to an Odor in Zebrafish. Curr. Biol. *24*, 1167–1175.

111. Benowitz, N.L., Dains, K.M., Dempsey, D., Herrera, B., Yu, L., and Jacob, P., 3rd. (2009). Urine nicotine metabolite concentrations in relation to plasma cotinine during low-level nicotine exposure. Nicotine Tob. Res. *11*, 954–960.

112. Borrego-Soto, G., and Eberhart, J.K. (2022). Embryonic Nicotine Exposure Disrupts Adult Social Behavior and Craniofacial Development in Zebrafish. Toxics *10*, 612.

113. Choi, H.M.T., Schwarzkopf, M., Fornace, M.E., Acharya, A., Artavanis, G., Stegmaier, J., Cunha, A., and Pierce, N.A. (2018). Third-generation hybridization chain reaction: multiplexed, quantitative, sensitive, versatile, robust. Development *145*, dev165753. https://doi.org/10.1242/dev.165753.

114. Cheng, R.-K., Krishnan, S., and Jesuthasan, S. (2016). Activation and inhibition of tph2 serotonergic neurons operate in tandem to influence larval zebrafish preference for light over darkness. Sci. Rep. *6*, 20788.

115. Cheng, R.-K., Tan, J.X.M., Chua, K.X., Tan, C.J.X., and Wee, C.L. (2022). Osmotic Stress Uncovers Correlations and Dissociations Between Larval Zebrafish Anxiety Endophenotypes. Front. Mol. Neurosci. *15*, 900223.

116. ZFIN: Zebrafish Book: Growing Zebrafish https://zfin.org/zf_info/zfbook/chapt3/3.3.html.

117. Zhang, S., 张思思, Chen, X., 陈旭, Jin, E., 金恩惠, Wang, A., 王安可, Chen, T., 陈婷婷, Zhang, X., 张小龙, Zhu, J., 朱军伟, Dong, L., 董丽莉, Sun, Y., 孙艳玲, Yu, C., 俞彩霞., et al. (2025). The GSA Family in 2025: A Broadened Sharing Platform for Multi-omics and Multimodal Data. Genom. Proteom. Bioinform. *23*, qzaf072. https://doi.org/10.1093/gpbjnl/qzaf072.

118. CNCB-NGDC Members and Partners (2025). Database Resources of the National Genomics Data Center, China National Center for Bioinformation in 2025. Nucleic Acids Res. *53*, D30–D44.

119. Goodman, W.M., Spruill, S.E., and Komaroff, E. (2019). A proposed hybrid effect size plus *p*-value criterion: Empirical evidence supporting its use. Am. Stat. *73*, 168–185. https://doi.org/10.1080/00031305.2018.1564697.

120. Ho, J., Tumkaya, T., Aryal, S., Choi, H., and Claridge-Chang, A. (2019). Moving beyond P values: data analysis with estimation graphics. Nat. Methods *16*, 565–566. https://doi.org/10.1038/s41592-019-0470-3.

121. Cliff, N. (1993). Dominance statistics: Ordinal analyses to answer ordinal questions. Psychol. Bull. *114*, 494–509. https://doi.org/10.1037/0033-2909.114.3.494.

122. Meissel, K., and Yao, E. (2024). Using Cliff's delta as a non-parametric effect size measure: An accessible web app and R tutorial. Pract. Assessment Res. Evaluation *29*, 2. https://doi.org/10.7275/PARE.1977.

STAR★METHODS

KEY RESOURCES TABLE

REAGENT or RESOURCE	SOURCE	IDENTIFIER
Antibodies		
Monoclonal anti-Tubulin antibody, beta, clone KMX-1	Sigma-Aldrich	Cat# MAB3408; RRID: AB_94650
Polyclonal anti-CHRNA5	Sigma-Aldrich	Cat# AV34967-100UG); RRID: AB_1854470
Polyclonal anti-mouse goat	DAKO	Cat# P0447; RRID: AB_2617137
Polyclonal Anti-rabbit	Santa Cruz Biotechnology	Cat# sc-2004 RRID: AB_631746
Chemicals, peptides, and recombinant proteins		
Nicotine hydrogen tartrate salt (≥ 99 %)	Sigma-Aldrich	Cat#6019-06-3
Ethanol (absolute)	Merck Millipore	Cat#1.00983.2511
DID fluorescent dye	Invitrogen	Cat#D7757
Trizol	Thermo Fisher Scientific	Cat#15596026
N-Phenylthiourea (aka. Phenylthiocarbamide)	Sigma Aldrich	Cat#P7629
Paraformaldehyde, 4% in PBS	Thermo Fisher Scientific	Cat#J61899.AP
Egg yolk from chicken	Sigma Aldrich	Cat#E0625
Protein rich diet	Customised Zebrafeed from Sparos (C. Wee Lab)	–
20x SSC Buffer	1st Base	Cat#BUF-3050-20X1L
1M Tris-HCl Buffer pH 7.4	Bio-Basic	Cat#USD8125
Sodium Chloride solution 5M	Sigma Aldrich	Cat#59222C
Ethylenediaminetetraacetic acid	Sigma Aldrich	Cat#EDS-500G
RNase Zap	Invitrogen	Cat#AM9784
10x Phosphate buffered saline (PBS)	1st Base	Cat#BUF-2041-10x1L
Acrylamide/Bis-Acrylamide solution 37.5:1, 30% w/v	Bio-Basic	Cat#A0011
TEMED	Bio-Rad	Cat#161-0801
RIPA buffer	Sigma Aldrich	Cat#R0278-50ML
Agarose	Bio-Basic	Cat#D0012
Dextran Sulfate	VWR chemicals	Cat#0198-50G
Ammonium persulfate	Bio-Basic	Cat#AB0072
Formamide	Sigma Aldrich	Cat#F7503-250ML
Citric Acid	Sigma Aldrich	Cat#0529-500G
Sodium Dodecyl Sulfate (SDS) Solution 20% w/v	1st Base	Cat#BUF-2052-1L
Tween 20 (polythene glycol sorbitan monolaurate)	Sigma Aldrich	Cat#P1379-250ML
Denhardt's Solution 50x	Invitrogen	Cat#750018
Diethyl Pyrocarbonate 96%	Sigma Aldrich	Cat#D5758-25ML
Heparin sodium salt from porcine intestinal mucosa	Sigma Aldrich	Cat#H3149-25KU
Critical commercial assays		
Abcam ethanol assay kit	Abcam	Cat# ab65343
Cotinine ELISA kit	Elabscience	Cat#E-EL-0064
GoTaq qPCR Master Mix	Promega	Cat#TM318
PureLink® Micro RNA Kit	Thermo Fisher Scientific	Cat#12183016
Pierce BCA Protein Assay Kit	Thermo Fisher Scientific	Cat#23225

(*Continued on next page*)

Continued

REAGENT or RESOURCE	SOURCE	IDENTIFIER
SuperScript II First-Strand Synthesis System	Invitrogen	Cat# 18091050
Deposited data		
RNA sequencing	The raw sequence data reported in this paper have been deposited in the Genome Sequence Archive (Genomics, Proteomics & Bioinformatics 2025) in National Genomics Data Center (Nucleic Acids Res 2025), China National Center for Bioinformation / Beijing Institute of Genomics, Chinese Academy of Sciences	(GSA: CRA032492) that are publicly accessible at https://ngdc.cncb.ac.cn/gsa.
Raw data for main and supplementary figures	Mendeley Data	DOI: https://doi.org/10.17632/y3nzn8pdmj.2
Experimental models: Organisms/strains		
Danio rerio (AB WT; *nacre* $^{-/+}$)	IMCB Zebrafish Facility	RRID: ZFIN_ZDB-GENO-960809-7
Oligonucleotides		
Custom primers for single-guide RNA template	Integrated DNA Technologies	N/A See Table 1 Main text for sequences
CAS9 mRNA (pT3TS-nCas9n)	Addgene	Cat#46757
Custom primers used for qPCR of *chrna5*, and housekeeping genes	Integrated DNA Technologies	N/A See Table 2 Main text for sequences
Custom probe cocktail sequences for HCR	Integrated DNA Technologies	N/A Refer to Table S1
B1 546 HCR Amplifier v3.0	Molecular Instruments, Inc.	–
B2 647 Amplifier v3.0	Molecular Instruments, Inc.	–
B3 488 Amplifier v3.0	Molecular Instruments, Inc.	–
Software and algorithms		
CRITTA (LabVIEW software for tracking)	Krishnan and Mathuru et al., 2014	http://www.critta.org (James Steward and Adam Claridge-Chang)
LabVIEW	National Instruments	RRID: SCR_014325
Behavioral tracking scripts (SAZA)	Raine et al., 2025 / GitHub	https://github.com/mechunderlyingbehavior/SAZA_2023
Fluorescence quantification code (EZgut)	Cheng et al., 2022 / GitHub	https://github.com/CarolineWeeLab/EZgut
Fiji (ImageJ)	Schindelin et al., 2012	RRID: SCR_002285
Olympus FV31S-SW	Olympus	RRID: SCR_017015
Partek Flow v11.0	Partek Inc.	RRID: SCR_011860
Python v2.7 + OpenCV library	Python Software Foundation	RRID: SCR_008394
R v4.4.2	R Project for Statistical Computing	RRID: SCR_001905
R studio v2025.09.2+418	Posit Software	RRID: SCR_000432
Tidyr (v1.3.1)	R Project for Statistical Computing	RRID: SCR_017102
Dplyr (v1.1.4)	R Project for Statistical Computing	RRID: SCR_016708
ggplot2 (v3.5.1)	R Project for Statistical Computing	RRID: SCR_014601
Lme4 (v1.1-37)	R Project for Statistical Computing	RRID: SCR_015654
lmerTest (v3.1-3)	R Project for Statistical Computing	RRID: SCR_015656
Emmeans (v1.11.1)	R Project for Statistical Computing	RRID: SCR_018734
DABEST (R v2025.3.14)	Ho et al., 2019	RRID: SCR_022340
Cocor (R v1.1-3)	Diedenhofen & Musch, 2015	http://comparingcorrelations.org
Snapgene	Dotmatics	RRID: SCR_015052
Geneious	Dotmatics	RRID: SCR_010519
AlphaFold Protein Structure Database	EMBL-EBI	RRID: SCR_023662
Adobe Illustrator 2025 (v29.5.1)	Adobe	RRID: SCR_010279
Biorender	Biorender	RRID: SCR_018361
CHOPCHOP	bio.tools	RRID: SCR_015723

(*Continued on next page*)

Continued

REAGENT or RESOURCE	SOURCE	IDENTIFIER
Others		
12–230 kDa Separation Module 13-capillary cartridge	ProteinSimple	Cat# SM-W002
LED Lightbox for SAZA (5000 lux)	Artograph	LightPad LX Series
Basler acA2040-90μM USB 3.0 camera	Basler	acA2040-90μM
Pinch-Valve solenoids	Automate Scientific	Cat#SKU:02-pp-04i
Silicone tubing 1/32in i.d. x 1/16in o.d.	Automate Scientific	Cat#SKU:05-14
Infrared LED bars, 24V, 850nm	TMS Lite	Cat#LBS2-00-080-2-IR850-24V
Arduino Nano 3.0 microcontroller boards	Arduino	SKU A000005
Cytation^{TM}3 Plate Reader	BioTek	CYT3MFV
Spark Microplate Reader	Tecan	RRID: SCR_021897
Microtube Homogenizer	Thomas Scientific	Cat#1191H97
Nanodrop 2000	Thermo Fisher Scientific	RRID: SCR_018042 Cat#ND2000
Applied Biosystems 7500 Real-Time PCR System	Applied Biosystems	RRID: SCR_018051
Applied Biosystems Veriti 96 well thermal cycler	Applied Biosystems	RRID: SCR_021097
WES system	ProteinSimple	Cat#004-600
Paramecium caudatum	Derived from Zebrafish International Resource Centre	–
Leica M205 FA fluorescent stereoscope	Leica	M205 FA
35mm glass bottom dishes no. 1.0 uncoated	Matek	Cat#P35G-1.0-20-C

EXPERIMENTAL MODEL AND STUDY PARTICIPANT DETAILS

Fish husbandry

Zebrafish (*D. rerio*, ABWT) were housed, bred, and reared at the Zebrafish Facility (ZFF, Institute of Molecular and Cell Biology, A*STAR) in groups of 20–30 in 3 L tanks at 28°C. Fish were kept under a 14:10 light dark cycle and fed as per the standard operating procedures of ZFF. All experimental protocols involving zebrafish were approved by the Institutional Animal Care and Use Committee (IACUC) of the Biological Resource Center at A*STAR. Approved experimental protocols (IACUC #201529, #231808, #231797) were followed. All experiments we performed on fish < 35 dpf, by which time sexual differentiation is not complete, and thus were not separated based on sex. At ∼30-35 dpf, the fish weighed between 10-25mg.

Generation of *chrna5* mutant zebrafish

Zebrafish gene editing by CRISPR-Cas9 is comprehensively described by Hwang et al.[109] In brief, CRISPR targets for *chrna5* were determined using the web tool 'CHOPCHOP' (https://bio.tools/chopchop) for the exon 8, targeting between the 3rd and 4th transmembrane helices to disrupt key functional domains. Primers for generating sgRNA are detailed in Table 1. Zebrafish embryos (nacre background) were injected at the 1-cell stage with 1 nL of a mixture containing 1 μL sgRNA (≈ 4-5 μg) and 1 μL Cas9 mRNA (≈1 μg). Fish were genotyped by fin-clipping and sequencing of genomic DNA at 10 weeks post-injection to identify founder fish (F0). The identified founder fish were outcrossed to AB background WT fish to obtain F1 embryos. F1 embryos from each outcrossed family were collected, and some of the embryos were genotyped. Once germline transmission was confirmed, the remaining embryos were grown to adulthood. Homozygous *chrna5* mutants from the F3 generation onwards were used for all subsequent experiments, henceforth referred to as *chrna5*$^{-/-}$. They were raised similarly as the WT fish.

METHOD DETAILS

Self-administration for zebrafish assay (SAZA) apparatus setup

Full descriptions of the tanks and apparatus used for the SAZA assay can be found in Nathan et al.[41] and Raine et al.[44] In brief, the assay tanks were constructed of 3mm thick opaque acrylic (dimensions: 35 x 75 x 30mm, width × length × height). One narrow end of the tank was divided by a sheet of the same material, 30mm in length, to split that end into two halves, while still permitting access by the fish (Figure 2A). The tank was placed on top of an LED lightbox, providing 5000 lux at maximum intensity (LightPad LX Series, Artograph, USA). Videos were captured at 30 frames per second using an acA2040-90μM USB3.0 Basler camera. Nicotine, alcohol, and control solutions were dispensed by gravity from 10ml syringes, mounted vertically an equal distance above the tank, through silicon tubing (outer diameter: 1/16'', inner diameter 1/32'') into the corner of their designated zone. Dispensing was mediated via

solenoid pinch valves, set to open only when a tracked fish entered the designated zone (Automate Scientific, USA, SKU: 02-pp-04i) (Figure 2A). Fresh system water was consistently supplied to the tank via additional silicon tubing at the opposite end of the tank to the stimulus/control delivery zones. Water was also removed from the tank at a matching rate (~2ml per minute) by gravitational siphoning, with the outflow tubing positioned at the end of the dividing sheet, outside the stimulus/control delivery zones (Figure 2A). This created a constant, gentle flow of water through the tank, while also preventing the dispensed solutions from escaping their designated zones (Figure 2A). Custom LABVIEW software, CRITTA (http://www.critta.org), was used to track fish movements as described by Krishnan et al. (2014).[110]

SAZA

The SAZA assay was performed as described by Nathan et al.[41] and Raine et al.[44] Each tank was filled with 40 ml of system water, with the system water inflow and outflow tubes, and the stimulus and control dispensing tubes, inserted into their respective positions. Juvenile zebrafish (30-35 dpf), naive to SAZA, were taken from the husbandry tanks, and one was added to each SAZA tank while minimising disturbance. Fish were given approximately five minutes to acclimate. Fish that did not swim freely throughout the chamber were rejected from further experimentation and replaced with a new fish. Closed loop tracking lasted for 24 minutes and consisted of three periods; three minutes of pre- and post exposure interspersed with an 18-minutes self-administration period where entry of the fish into the stimulus or control zones triggered dispensing of the corresponding solution (Figure 2A). The stimuli delivered were 0/5/10/20% of absolute alcohol, or 0/10/500μM nicotine hydrogen tartrate salt (cat #6019-06-3 Sigma) diluted in system water. These source concentrations are diluted with the concentration increasing over time. As outlined in Table S2, this was estimated to be ~10-40 fold dilution with nicotine, and measured at ~25 to ~70 fold with alcohol.[44] This resulted in average concentrations of $\bar{x}$0.125/$\bar{x}$0.25/$\bar{x}$0.5% for alcohol and of $\bar{x}$0.5/$\bar{x}$25 μM for nicotine, respectively. The volume of each stimulus or control dispensed by each fish was recorded. Experimenters were not blinded. However, several steps were taken to reduce experimental bias. Each experimental condition was staggered and was interspersed over multiple months such that both genotypes were examined every week. Each experiment was performed using multiple mixed clutches of fish to avoid batch effects. Following each cycle of experimentation, the chamber was cleaned, rinsed, and refilled with fresh tank water. The zone designated to deliver the stimulus solution was psuedo-randomly assigned to be either the left or the right zone, such that ~50% of the fish were tested in each configuration. The same apparatus was used for all experiments. Approximately 30 fish were assayed per concentration of alcohol or nicotine. Following each assay, the fish were euthanized.

In some cases, zebrafish were pre-treated with exposure to alcohol or nicotine solutions before being assayed. For these assays, fish were immersed in either system water (0μM/0%), 1μM nicotine, or 1% alcohol, diluted in system water, for one hour for seven consecutive days. Following this pre-treatment, these fish were returned to the facility for usual husbandry. On the eighth day, the fish were subjected to SAZA, either using the same substance as introduced during pre-treatment, or the opposite, creating four total conditions (Figure 3A).

Body alcohol/cotinine quantification

Juvenile zebrafish (30-35 dpf) were taken directly from husbandry tanks and introduced to smaller tanks containing 10ml system water, three fish per tank. To each tank, 10ml of 2x the desired drug solution (alcohol: 0%/0.5%/1.5%, nicotine: 0μM, 25μM, 50μM) was added, and the timer started. Following immersion for the designated times for alcohol (1, 2, 3, 18 minutes), the fish were briefly rinsed in system water and euthanized by hypothermic shock. Upon confirmation of death, the fish were thoroughly rinsed in Milli-Q water to remove trace drug from the skin, and frozen on dry ice until tissue homogenisation. For nicotine, after immersion (3, 18 minutes), the fish were briefly rinsed in system water and transferred to new tanks containing no nicotine for 24 hours to allow metabolism of nicotine to cotinine. These fish were then subsequently euthanised as described above.

For body alcohol quantification, each fish was weighed, and then homogenised in 1.5ml Eppendorf tubes by pellet pestle, in 50mM Tris-HCL with volume equivalent to 10x the weight of the fish, assuming the fish tissue density was equal to water (e.g. 90uL buffer per 10mg/uL fish). The homogenate was centrifuged at 14,000 rpm for 20 minutes at 4°C, and the supernatant was extracted. The supernatant was centrifuged again under the same conditions for 10 minutes, and the supernatant stored at -80°C until use.[51] Body alcohol content was quantified using Abcam ethanol assay kit ab65343, at 570nm on a Cytation 3 plate reader (BioTek).

Quantitative analysis of cotinine, a primary metabolite of nicotine, is used to estimate the body burden of nicotine in smokers.[111] We adapted a method that was previously used to quantify nicotine exposure in zebrafish embryos.[112] Briefly, fish were weighed and homogenized in 1.5 ml Eppendorf tubes using a mechanical homogenizer. Samples were submerged in 150 μl RIPA buffer and then brought up to a final volume of 200 μl. The homogenate was centrifuged at 14,000 rpm for 20 minutes at 4°C, and the supernatant was transferred to a new tube for immediate use. Cotinine levels were measured using the cotinine ELISA kit (Elabscience, #E-EL-0064) according to the manufacturer's instructions and corrected for dilution. Absorbance readings at 450 nm and 540 nm were obtained using a Spark microplate reader (Tecan). Each biological replicate was assayed in triplicate.

RNA extraction

Juvenile zebrafish (28dpf) were euthanized following the pretreatment scheme (Figure 3), and the brains were dissected in 1x PBS pH 7.0 to exclude the olfactory bulb (OB), telencephalon (TEL), and hindbrain (HB) regions. The dissected brain tissue was homogenised using a microtube homogenizer (Thomas Scientific) in a Trizol lysis buffer (ThermoFisher #15596026). RNA was then extracted using

PureLink® Micro RNA Kit (ThermoFisher #12183016) according to the manufacturer's protocol. The concentration and purity of the extracted RNA were determined by NanoDrop™2000 Spectrophotometer (ThermoFisher). Each brain sample yielded around 100 ng/μL RNA with a ratio of absorbance reading 1.9-2.0 at 260/280 nm. Some RNA samples were sent for bulk sequencing, detailed below. The remaining purified RNA was reverse transcribed by SuperScript II First strand Synthesis System (Invitrogen #18091050) using 100 ng/μL of purified RNA to obtain approximately 1000 ng/μL of first strand cDNA. Negative controls containing no reverse transcriptase were set up for each sample to check for genomic DNA contamination. The cDNA was diluted with nuclease-free water to 100 ng/μL and used for qRT-PCR.

qRT-PCR

The qRT-PCR amplification mixtures (20 μL) contained 100 ng of cDNA, 10 μL 2x GoTaq®qPCR Master Mix (Promega #TM318), and 300 nM forward and reverse primers. The primers used were designed using Primer3 (v.0.4.0) and are detailed in Table 2.

Reactions were performed using an Applied Biosystems 7500 Real-Time PCR system, in 96-well plate format. The cycling conditions were as follows: 95°C for 10 m to activate, then 40 cycles of 95°C for 15s, 60°C for 30s. After completion, a melt curve was run at 65-95°C for 5 seconds per step. All PCR efficiencies were between 90-110%. Primer specificity was validated by a single peak on the post-PCR melt curve and single-band after electrophoresis. The relative gene expression levels were normalised to the housekeeping genes and analysed using the adjusted delta-delta CT method, described by Hellemans and Mortier et al. (2007). All data were analysed as described below.

Hybridisation chain reaction, RNA-fluorescent in-situ hybridisation (HCR™ RNA-FISH)

Larval zebrafish for HCR™ RNA-FISH 3.0 (HCR)[113] were collected as follows. During development, 300μL of 0.3% PTU (Phenylthiocarbamide, Sigma) was added to each petri dish containing larvae every other day from 3 dpf until 14 dpf to reduce pigmentation. Following this, larvae were quickly rinsed with 1x PBST, euthanized, and fixed in 4% formaldehyde, diluted in 1X PBST, at room temperature for 60 minutes with shaking. Once fixed, the larvae were washed with 1X PBST for three minutes, three times. Larvae were then permeabilized using a detergent solution (1% SDS, 0.5% Tween 20, 150mM NaCl, 1mM EDTA, 0.05M Tris-HCL, pH 7.5) at 37°C for 30 minutes and washed for three minutes, three times each with 1X PBST and then 5X SSCT. Finally, the larvae were transferred to 30% probe hybridization buffer (30% formamide, 9mM citric acid, 0.1% Tween 20, 50μg/mL heparin, 1x Denhardt's solution, 5X SSC) and incubated at 37°C for 30 minutes. At this stage, the larvae were stored at 4 degrees for up to one month in the dark or used directly for HCR.

HCR probes against *chrna5*, *neurod1*, and *nrp1a, slc17a7a, slc17a6b, kiss1, gpr139, grinaa, and grin2ba* were prepared using an in-house Excel-based program and synthesized by IDT (see Table S1 for details). Probes were prepared in a cocktail containing 30ul (10 μM) of each probe set against each gene in 1000 μl of 30% probe hybridization buffer. The in-situ hybridization experiments were carried out in an automated robotic fluidics system. The larvae were transferred to the automated fluidics robot with the primary, secondary, and wash buffers, and a script to perform the reaction was loaded (preprogrammed in the system). The larvae were first incubated with the probes at 37°C for 8 hrs, then washed five times with 30% probe wash buffer (30% formamide, 9mM citric acid, 0.1% Tween 20, 50μg/mL heparin, 5x SSC) at 37°C and then 5X SSCT twice. For the secondary reaction, HCR hairpins diluted and prepared in an amplification buffer (5X SSC, 0.1% Tween 20, 2.5% dextran sulphate) were added and incubated for 3 hours in the dark in the automated system. The larvae were then washed with 5X SSCT, eight times, for 2 mins each. After the reaction, the samples were removed from the chamber and mounted with the cover slip on the dorsal side in 70% glycerol-based mounting media and imaged on an Olympus FV3000 confocal microscope with the settings consistent between fish. Images were post-processed first on Olympus viewer FLUOVIEW FV31S-SW software with linear intensity adjustments of 150 - 4095 for all genes. Images presented for *nrp1a*, *neurod1,* and *chrna5* had no further processing beyond cropping to the ROI and addition of scale bars.

Protein extraction

Protein was extracted from the brains of adult fish, aged 6 months. The fish were euthanized, then subsequently dissected in 1x PBS pH 7.0. Brain tissue was transferred to 400 μl of cold, 6 M urea buffer with added protease inhibitors, and homogenized until the solution was clear of visible debris. The protein samples were then briefly vortexed and centrifuged for 30 seconds to pellet debris. The samples were then sonicated with three 30 second pulses at one minute intervals using a probe sonicator on ice. The samples were then incubated on ice for 20 minutes before centrifuging at 14,000 rpm for 20 minutes at 4°C. The supernatant was then transferred to a new tube, aliquoted, and stored in -80°C until further use. Protein concentrations were measured using the Pierce BCA Protein assay kit (Thermo Fisher Scientific), following the manufacturer's protocol in 96 well plate format. BSA standards were serially diluted in 6M urea buffer from a working concentration of 2000 μg/ml to 25 μg/ml to create a standard curve. In each well, 25 μl of diluted BSA standard or protein sample was added, and each topped up by 200μl of BCA working solution. The plate was covered and incubated for 37°C for 30 minutes, before absorbance at 562 nm was determined by a plate reader. From one round of protein extraction, approximately 0.8 mg/ml was extracted.

Western blot

Western blots were performed on extracted brain proteins by Wes system (ProteinSimple, product number 004-600) using a 12-230 kDa Separation Module 13-capillary cartridge SM-W002. Samples were diluted to 1 μg/μL in 6 M urea buffer, mixed in fluorescent 5x Master Mix, including DTT, and denatured at 95°C for five minutes. The samples, primary antibodies (1:1000 diluted in Wes antibody diluent),

HRP-conjugated secondary antibody (1:4000 diluted in Wes antibody diluent), and chemiluminescent substrate (luminol-S and peroxide) were added onto the plate, in addition to the biotinylated ladder, antibody diluent, and wash buffer included on the plate by the manufacturer. Default instrument settings were used, stacking and separation at 475V for 30 minutes, blocking 5 minutes, primary antibody incubation, 60 minutes, and secondary antibody incubation, 30 minutes. The chemiluminescence detection was set for 30 minutes total, with imaging at 2-minute intervals. The electropherograms were first checked to see if manual correction was needed for peak detection, and then the band intensity results were exported. Visualization of bands was generated digitally by the Wes system based on peak intensity. The following primary antibodies were used: for the reference protein, monoclonal anti-Tubulin antibody, beta, clone KMX-1 (MAB3408) Sigma, produced in mice. For *chrna5*, Monoclonal anti-CHRNA5 antibody (AV34967-100UG) Sigma, produced in rabbit, Table 2.3.3.3. The secondary antibodies used were polyclonal anti-mouse goat antibody (P0447 DAKO) HRP conjugated, and polyclonal Anti-rabbit (sc-2004 Santa Cruz Biotechnology), produced in goat HRP Conjugated.

Light/dark preference assay

The light/dark preference assay, designed to test nyctophobia/photophila as a proxy for anxiety, was set up and performed as described by.[61] Four transparent rectangular plastic boxes (70mm x 40mm x 15mm, L x W x H) were each filled with 50ml of system water. The boxes were placed inside a cabinet, covered with a cloth to prevent any light interference. Each box was divided into light and dark sides, each 35 mm in length, by using an iPad (Apple 7th generation, display at highest light intensity) underneath to project an equal light/dark split image (Figure 6A). A camera (ACa2040-90 uM USB 3.0: Basler resolution 800 x 600 pixels) with an infrared filter was placed overhead, which recorded the movements of 12-14 dpf larvae. To prevent social interference, dividers were placed between the four chambers to isolate the fish completely. The setup was further illuminated by placing two infrared LED bars on either side of the tanks (Figure 6). The camera output was recorded using Pylon viewer Ver 6.1.1. All trials were conducted between 9am-6pm. Prior to the assay, larvae were either not treated with any stimulus. The larvae were quickly and gently added to the illuminated rectangular boxes, with one larva per box, four boxes at a time. A total of ~36 individuals per treatment and genotype were assayed. Larvae were allowed to acclimate in the chamber for ten minutes until free, uninhibited swimming was observed before starting the video recording. Then, the larvae were filmed for ten minutes in complete light, followed by a further ten minutes in the light and dark setting (Figure 6A). Each fish was tracked in real time by an in-house custom-written Python code using the opencv library.[114] Each recording lasted 10,000 frames at 16 fps, totalling approximately 10 minutes. The x-y coordinates of each larva in each frame were exported. Automated analyses[114] were applied to all larvae, however, individuals that moved less than 50 mm during the total assay duration were excluded from the final data. Experimenters were not blinded, and the position of genotypes was randomised throughout the experiment. Planned contrasts were assessed between genotypes for total time spent in the dark, and the number of entries into the dark. Further exploratory analyses were conducted to compare the first entry into the dark.

Circadian rhythm assay

The circadian assay was performed in 48-well plates, with each well containing 1ml of system water. These plates were placed inside an opaque rectangular box to avoid outside light interference, on top of an illuminated light box, surrounded by four IR LED bars (LBS2-00-080-2-IR850-24V, 850nm: TMS Lite). A camera (Aca2040- 90μM USB 3.0: Basler) with an IR filter was positioned above the plate to track the movement of each 7-10 dpf larva. At the onset of recording, ~15:00-15:30 pm, the larvae were kept in continuous ambient light. The illumination was switched off at 22:30, and switched on again at 08:30 the next day, and the assay ended after 24 hours. Larval movements were tracked by an in-house custom-written script in Python 2.7,[115] incorporating functions from the OpenCV library to control the Arduino microcontroller and video track larvae movement. Videos were captured at 576 x 854 px at 10 fps, and the background subtraction method was applied to obtain the X and Y coordinates of the fish. The protocol is further described in detail in.[115] The following key metrics were quantified: total seconds spent moving per minute, mean velocity, mean resting period, and average distance moved per fish. Activity thresholds were defined as such: an active bout was indicated when the larvae moved for five seconds or more per minute. Meanwhile, a resting, or inactive bout, was indicated when larvae moved for four seconds or less for one minute. For the assay duration, larvae were either not treated with any stimulus. Two other behavioural assays were also conducted during the circadian assay duration, testing the startle responses to light/dark, and to vibration. The light/dark startle response test occurred for five, 30 minute light/dark cycles for a total of five hours, from ~17.30 – 22.30 pm (Figures 6J–6L). The vibration test consisted of six, 20 minute cycles, two per hour. Within these cycles, 18 shocks were administered per hour for nine different intensities, first from 0-100% ascending, and subsequently descending, from a period of ~1:00-7:00 am (Figure 6I). Vibrations were controlled through a speaker via an Arduino microcontroller board by a custom Python script (Python 2.7, C.[115] The highest intensity was represented by 50% on the computer audio output. The time interval between each vibration was 30 seconds, which prevented behavioural habituation. The larvae were recorded as responding if they moved more than 7 pixels (~ 4 mm), and the average percentage of responding fish was calculated for each different intensity. The observed values were corrected against baseline locomotor activity, as further described by.[115] For each fish, the data points from all cycles were averaged together prior to statistical analysis. Individuals that moved less than 50 mm during the total assay duration were excluded from the final data. Experimenters were not blinded, and genotypes were placed in alternating rows on the 48 well plates, with the first being randomised. Planned contrasts were assessed for total time inactive in evening, night, and morning, within and between genotypes, distance travelled in response to vibration between genotypes, and locomotor activity change within and between genotypes in response to light/dark transitions.

Feeding assay

Food types for the various feeding assays were prepared as follows. *Paramecium caudatum* was cultured and harvested weekly as described in the zebrafish book,[116] and '*Paramecium* Recipes for Large and Small Facilities'. Briefly, paramecia culture supernatants were collected in a clean 50 ml falcon tube to remove any yeast accumulated at the bottom, then centrifuged (Eppendorf) at 4°C, 15 minutes, 2500 rpm to isolate the pellet. The resulting supernatant was removed, and the paramecia pellet was resuspended in 1 mL of system water. Next, 2.5 μL of stock DID dye (Invitrogen) in 22.5 μL 100% ethanol was added to the resuspended paramecia and incubated for two hours at RT under nutation. Subsequently, the mixture was centrifuged at 13,000 rpm for five minutes at RT. The alcohol supernatant was removed, and the pellet resuspended in 1mL of system water under nutation for 15 minutes. The mixture was then briefly vortexed and added onto the rotator again for a further ten minutes to thoroughly mix the paramecia with the system water. Finally, 1mL of this dyed paramecia solution was added to 3 mL of system water and used to feed four plates of larvae (1 mL per plate). Egg yolk from chicken (#cat E0625 Sigma) was purchased and prepared as described for the paramecia, but with the following adjustments. For egg yolk powder, 10mg was measured and mixed with 1ml of system water and 1 μL DID stock dye. The tube was vortexed and incubated for 2 hours at RT under nutation. Subsequently, the supernatant was removed, without disturbing the pellet. The pellet was then resuspended in 1 ml of system water under nutation for 15 minutes, ready for use. The protein-rich powder, custom formulated and a gift from Caroline Wee lab, was prepared in the same manner as the egg yolk powder.

To perform the assay with paramecia, the larvae were subjected to two "training days" of feeding in the assay petri dish with 1ml of paramecia (30-40 larvae per petri dish) overnight. The assay was performed at 7 dpf. Larvae were first fed with excess unlabelled paramecia for 90 minutes during the first feeding session, then washed and fasted for 120 minutes. After the fasting period, the larvae were transferred into smaller, 35mm petri dishes, each filled with 4 mL of system water, before adding 1 mL of labelled paramecia. Larvae were given 90 minutes for the second feeding session, after which they were euthanized by hypothermic shock and fixed in 4% PFA in 1x PBST overnight at 4°C. Larvae were washed three times in 1x PBST the next day before mounting and imaging (Figure 6M). Experimenters were not blinded, genotypes were separated and treated in parallel.

The assay was performed in a similar manner with egg yolk or protein-rich powder as the food, but with the following adjustments. On the training days at 5 and 6 dpf, the fish were instead fed with a small quantity of 150/250 micro ground dry algae (Zeitger) for 30 minutes. The algae were then washed away, and replaced with fresh system water overnight. At 7 dpf, the first feeding session lasted for only 30 minutes, before the fasting period of 2 hours. For the second feeding session, 500μl of labelled-egg yolk, or protein rich powder, was added in petri dishes for 30 minutes, before fixing. To prepare for imaging, the fixed larvae were washed three times in 1x PBS and arranged per genotype (25-30 fish) in a 35mm glass bottom dish in a circular pattern, avoiding larvae touching each other. To measure the amount of food consumed by larvae, the intestinal fluorescence signal was captured using a Leica M205 FA fluorescent stereoscope. Corresponding brightfield and fluorescent images were captured, Cy5 filter 651 nm, in a covered, dark room. The brightfield images were captured at 20 ms exposure at 40% intensity, whilst Cy5/mcherry exposure was 100ms, 100% intensity. The fluorescence intensity was measured by an in-house written code developed by Cheng et al.,[115] which correlated to the total amount of food consumed by each larva. The segmentation method used for fluorescence quantification has been described in full by,[115] and the code is maintained and can be found at GitHub: https://github.com/CarolineWeeLab/EZgut.[115] The mean fluorescence intensity was obtained for each larva and normalized against the controls. Individuals that did not show any fluorescence in the gut were discarded from the study. Planned contrasts were made between genotypes within food types.

QUANTIFICATION AND STATISTICAL ANALYSIS

SAZA data quantification and analysis

CRITTA tracking data from SAZA were processed by custom Python scripts. These provided data on time spent in each zone, mean velocity in each zone, number of entries, and mean time per entry used in these analyses. The data were separated into three major time groups; pre-exposure, total stimulus delivery period, and post-exposure. The preference index was calculated for the total stimulus delivery period, based on the volume of each solution dispensed, by the following formula; PI = (VolS - VolC) / (VolS + VolC), where VolS = volume dispensed in stimulus zone (ml) and VolC = volume dispensed in control zone (s). This gives the value for PI a maximum range of + or - 1, indicating more volume dispensed, relative to the total, in the stimulus or control, respectively. For example, a PI of +1 would indicate 100% of the total volume dispensed was in the stimulus zone during the assay, while a PI of 0 would indicate equal volumes were dispensed in each zone. The comparisons of these parameters between genotypes and within genotypes under these time groupings were planned contrasts. Fish that were deemed not to have meaningfully interacted with the assay by not entering both stimulus and control zones were removed from the analysis. As a further exploratory analysis, the stimulus delivery period was also subdivided into three minute segments (0-3m/3-6m/6-9m, and so forth). Analysis scripts are available from Github (https://github.com/mechunderlyingbehavior/SAZA_2023).

RNAseq

The quality of each RNA sample was verified before sequencing by gel electrophoresis and bio-analyser. Samples that passed QC were sent for sequencing by BGI. An mRNA cDNA library made up of paired-end sequencing reads of 150 bp in length was generated on the Illumina HiSeq instrument. Raw reads were first processed to remove adapters, poly-N sequences, and reads with low quality from the raw data. All downstream analyses were based on the clean data with a Phred score of 39, indicating a 99.9% base call

accuracy. Further analysis was performed in Partek™ Flow™ Explore Spatial Multiomics Data using Partek™ Flow™ software, v11.0. Reads were aligned to GRCz11 genome assembly by STAR aligner, default parameters, and subsequently filtered to a minimum mapping quality score of > 30. Gene counts were normalised by median ratio, followed by differential expression analysis in DeSeq2. Significance thresholds were set as follows for exploratory analysis of the transcriptomic data: up/down-regulated genes = $p < 0.05$ & fold change > ±2. Provisional up/down-regulated genes = $p < 0.05$ & fold change < ±2. Non-significant genes = $p > 0.05$. Custom gene lists and sets for analysis can be found in Table S17. Gene set enrichment analysis (GSEA) was performed using the GRCz11-GO database, 100 permutations. Significance thresholds were set at $p < 0.05$ and FDR < 0.25. The raw sequence data reported in this paper have been deposited in the Genome Sequence Archive[117] in National Genomics Data Center,[118] China National Center for Bioinformation/ Beijing Institute of Genomics, Chinese Academy of Sciences (GSA: CRA032492) that are publicly accessible at https://ngdc.cncb.ac.cn/gsa/search?searchTerm=CRA032492.

Statistical analyses

Data in this study were analysed and presented following the principles of hybrid effect size plus *p* value.[119,120] Briefly, a P value as a measure of significance is improved upon by the supplementary reporting of effect sizes, means, and 95% confidence intervals.[120] The assumptions of homoscedasticity and normality typically recommended for parametric testing were not met consistently for the SAZA data. As such, unpaired data were compared by non-parametric Cliff's delta effect size and two-sided permutation T-tests (5000 reshuffles) with a significance level of 0.05. Repeated measures data were compared by mean difference and paired permutation tests under the same parameters. Vibration assay longitudinal data were analysed using a linear mixed effects model, with pixels travelled as the response variable, genotype and vibration intensity as fixed effects, and individual ID as a random effect to account for repeated measures. Analyses were performed in R using the 'dabestr' (v2024.12.24) and 'lmerTest' (v3.1-3) packages. If multiple comparisons were made, family wise error was corrected for by applying the Holm-Bonferroni step down method to *p*-values. The outputs of these statistical analyses can be found in supplementary tables. Where data were presented as Gardner-Altman and Cummings estimation plots, the results are reported as Cliff's delta, or Paired mean difference = X, 95% CI [lower, upper], $p = Y$. For Cliff's delta, effect sizes greater than ± 0.4 and a *p*-value of < 0.01 were considered meaningful and practically relevant in this study. Smaller Cliff's delta effect sizes of ± 0.2 to 0.4 with accompanying *p*-value of < 0.05 were considered provisionally meaningful, pending reproduction or further investigation.[119,121] The power target for each experiment was 80%, based on an expected effect size of 0.7 (0.7 Cohen's D = ∼0.43 Cliff's Delta[122]) and alpha of < 0.05. A sample size of 34 is estimated to achieve this target. Where smaller effect sizes were expected, or younger larvae were used, the sample sizes were increased accordingly.